The Inside & Outside of Top Jets

Gilad Perez

Weizmann Institute of Science

L. Almeida, S. Lee, G. Sterman, I. Sung, & J. Virzi (08);

L. Almeida, S. Lee, I. Sung, & J. Virzi (08);

S. Lee, A. Weiler & J. Zupan, in preparation.

Discussions with L. Almeida, S. Lee, J. Maldacena & G. Sterman.

Outline

- (very brief) Intro' top jets at the LHC.
- The nature of the problem (finite resolution).
- Semi-analytical results: jet mass+substructure => understand phys. (S vs. BG), drives new approach.
- Efficient algorithm (manifestly IRC-safe) exploiting fully & partially collimated regions.
- Systematic analysis fully col' & beyond t-jets ?
- Summary.

High p_t tops, might be crucial signal for various NP models

Z': Butterworth, Cox & Forshaw; KK gluon: Agashe, Belyaev, Krupovnickas, GP & Virzi (06); Lillie, Randall & Wang (07); KK graviton: Fitzpatrick, Kaplan, Randall & Wang (07); Agashe, Davoudiasl, GP & Soni (07).

$$M_{KKG} = 3\,\mathrm{TeV}$$

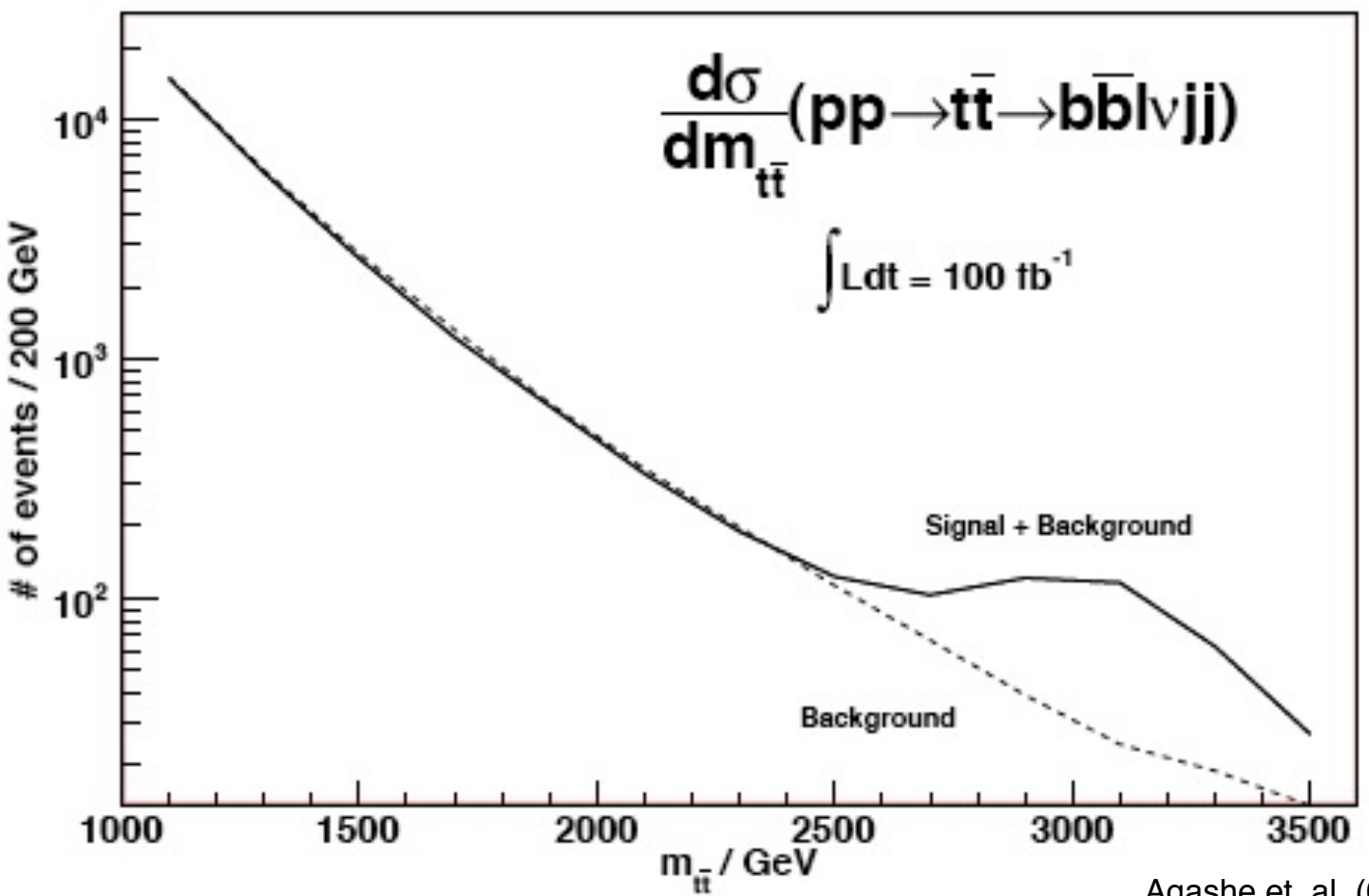

Agashe et. al, (06)

Why not use scaled-down conventional methods?

- IRC (IR & collinear) safety require inclusive observables (e.g. cone or k_t jets).
- Hadronic calorimeter tower has an hard angular size R~0.1.
- Radial shower of energetic hadrons are very large.

Shower size of a single 100 GeV pion

- Ave' cone of 20 cm is required to contain 95% of the energy; a full cell size!

E% vs. size of section

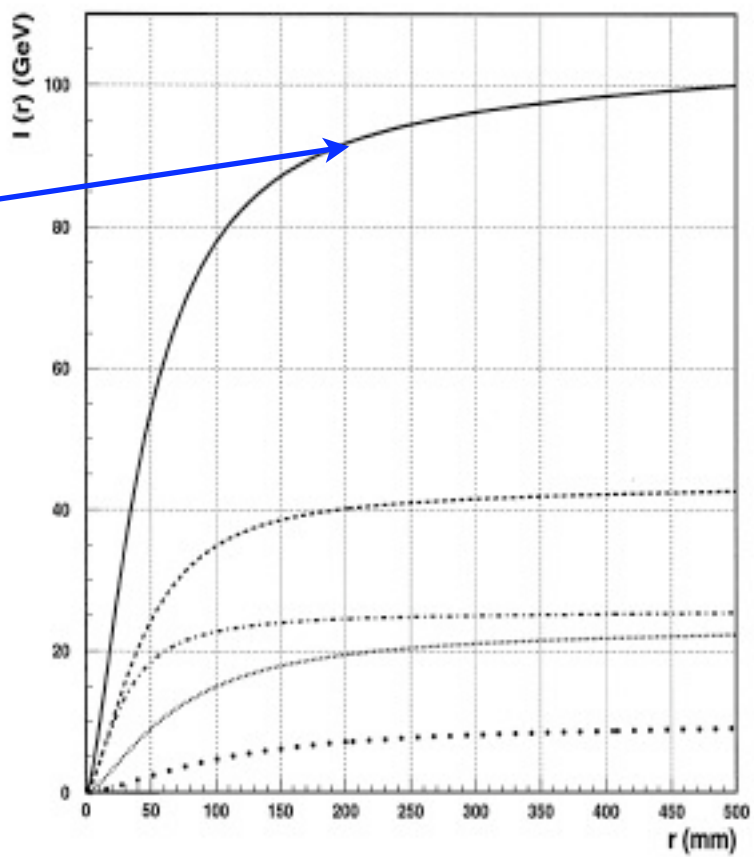

Fig. 14. Containment of shower $I(r)$ (the solid line) as a function of radius for the entire Tile Calorimeter. The dash-dotted line is the contribution from the first depth segment, the dashed line is the contribution from the second depth segment, the thin dotted line is the contribution from the third depth segment, the thick dotted line is the contribution from the fourth depth segment.

ATLAS, NIM A 443 (2000)

Shower size of a single 100 GeV pion

- Ave' cone of 20 cm is required to contain 95% of the energy; a full cell size!

- R=0.4 smallest cone used so far. A careful th'+exp' effort required to go beyond that.

E% vs. size of section

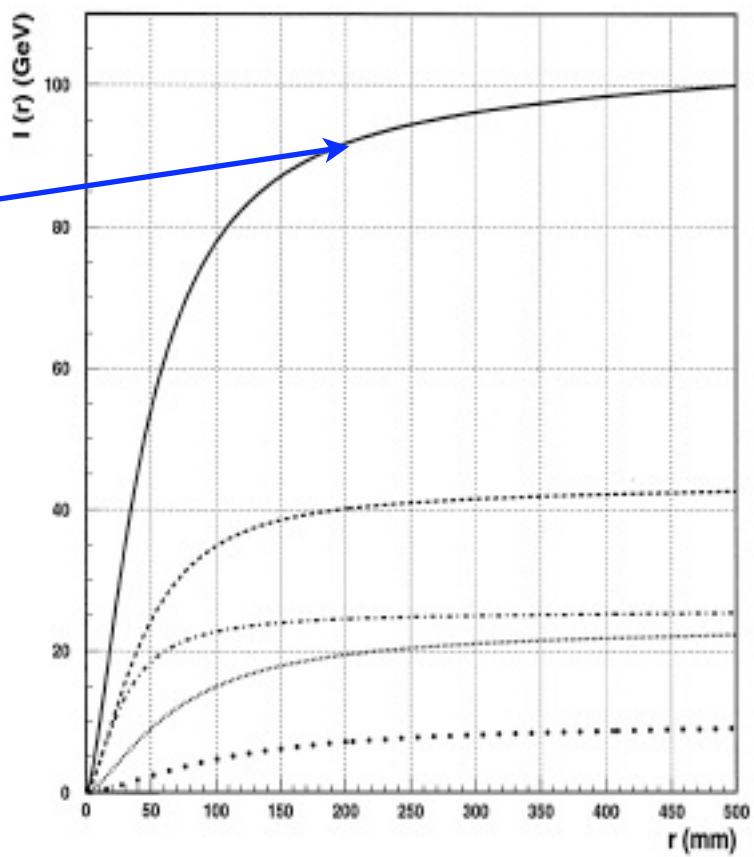

Fig. 14. Containment of shower $I(r)$ (the solid line) as a function of radius for the entire Tile Calorimeter. The dash-dotted line is the contribution from the first depth segment, the dashed line is the contribution from the second depth segment, the thin dotted line is the contribution from the third depth segment, the thick dotted line is the contribution from the fourth depth segment.

ATLAS, NIM A 443 (2000)

Shower size of a single 100 GeV pion

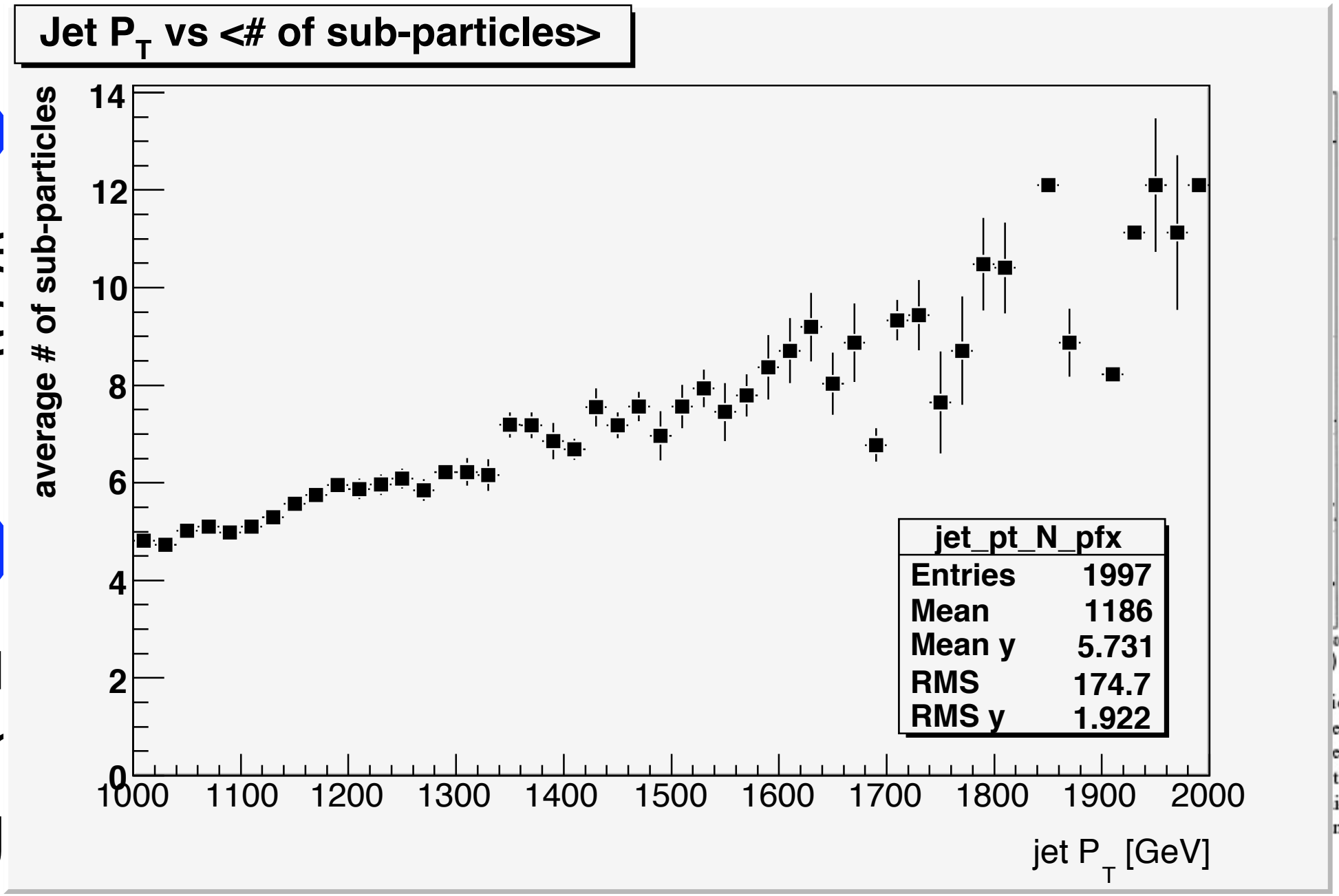

t-jets & di-jets @ the LHC

S/B < 10^{-2}, for pt(j)>1000GeV, R=0.4

(10pb for jj+X, 100fb for ttbar+X)

Almeida, Lee, GP, Sung, & Virzi.

Process	Generator	PDF	Matching	Cross Section
$pp \to t\bar{t}(j)$	SHERPA 1.0.9	CTEQ6M	CKKW	135 fb
$pp \to t\bar{t}(j)$	SHERPA 1.1.2	CTEQ6M	CKKW	149 fb
$pp \to t\bar{t}(j)$	MG/ME 4	CTEQ6M	MLM	68 fb
$pp \to t\bar{t}(j)$	MG/ME 4	CTEQ6L	MLM	56 fb
$pp \to t\bar{t}$	Pythia 6.4	CTEQ6L	-	157 fb
$pp \to t\bar{t}$	Pythia 8.1	CTEQ6M	-	174 fb
$pp \to jj(j)$	SHERPA 1.1.0	CTEQ6M	CKKW	10.2 pb
$pp \to jj(j)$	MG/ME 4	CTEQ6L	MLM	8.54 pb
$pp \to jj(j)$	MG/ME 4	CTEQ6M	MLM	9.93 pb
$pp \to jj$	Pythia 6.4	CTEQ6L	-	13.7 pb
$pp \to jj$	Pythia 8.1	CTEQ6M	-	13.3 pb

"Theory" of massive jets @ the LHC

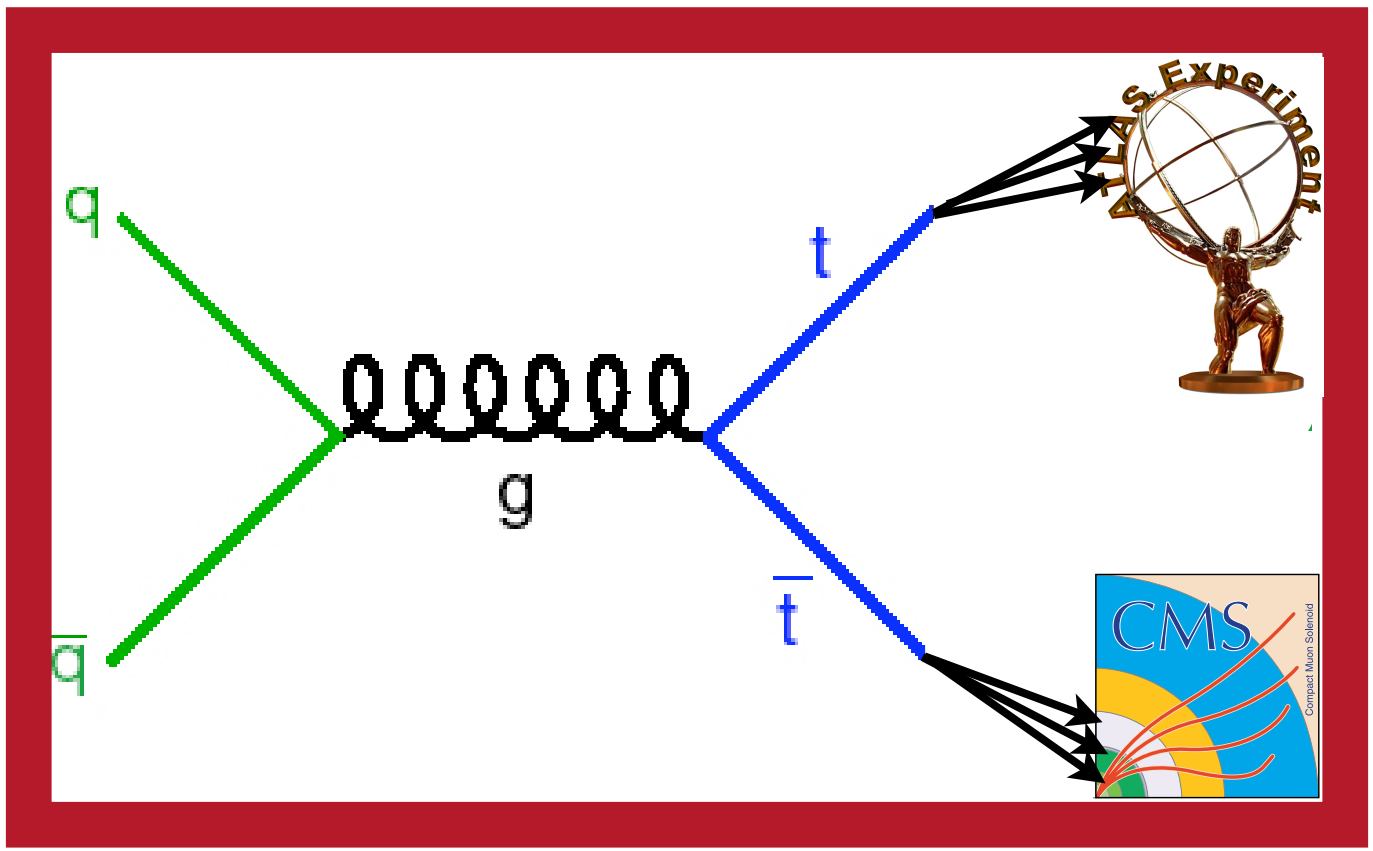

(I) Jet mass.

(II) Jet substructure:

(i) 2-body intuition (ii) angularity (iii) planarity.

Jet Mass, Overview

- Jet mass-sum of "massless" momenta in h-cal

  inside the jet: $m_J^2 = (\sum_{i \in R} P_i)^2, \; {P_i}^2 = 0$

- Jet mass is non-trivial both for S & B.

  (naively: QCD jets are massless while top jets ~ m_t)

Jet Mass, Overview

- Jet mass-sum of "massless" momenta in h-cal inside the jet: $m_J^2 = (\sum_{i \in R} P_i)^2, \; Pi^2 = 0$
- Jet mass is non-trivial both for S & B.
- Simple mass tagging fails. (counting in mass window)
- S&B distributions via 1st principles & compare to Monte-Carlo.
- Allow to improve S/B & yield insights!

Non trivial cone t-jet mass distribution

- Naively the signal is $J \propto \delta(m_J - m_t)$
- In practice: $m_J^t \sim m_t + \delta m_{QCD} + \delta m_{EW}$

Non trivial cone t-jet mass distribution

- Naively the signal is $J \propto \delta(m_J - m_t)$
- In practice: $m_J^t \sim m_t + \delta m_{QCD} + \delta m_{EW}$

Can understood perturbatively fast & small~10GeV

Non trivial cone t-jet mass distribution

- Naively the signal is $J \propto \delta(m_J - m_t)$
- In practice: $m_J^t \sim m_t + \delta m_{QCD} + \delta m_{EW}$

Can understood perturbatively fast & small~10GeV

Pure kinematical bW(qq) dist' in/out cone longer~0.2GeV

Non trivial cone t-jet mass distribution

- Naively the signal is $J \propto \delta(m_J - m_t)$
- In practice: $m_J^t \sim m_t + \delta m_{QCD} + \delta m_{EW}$

Can understood perturbatively fast & small~10GeV

+ detector smearing.

Pure kinematical bW(qq) dist' in/out cone longer~0.2GeV

Non trivial cone t-jet mass distribution

(Fleming, Hoang, Jain, Mantry, Scimemi, Stewart) Almeida, Lee, GP, Sung, & Virzi.

Sherpa => (CKKW) Transfer functions, JES

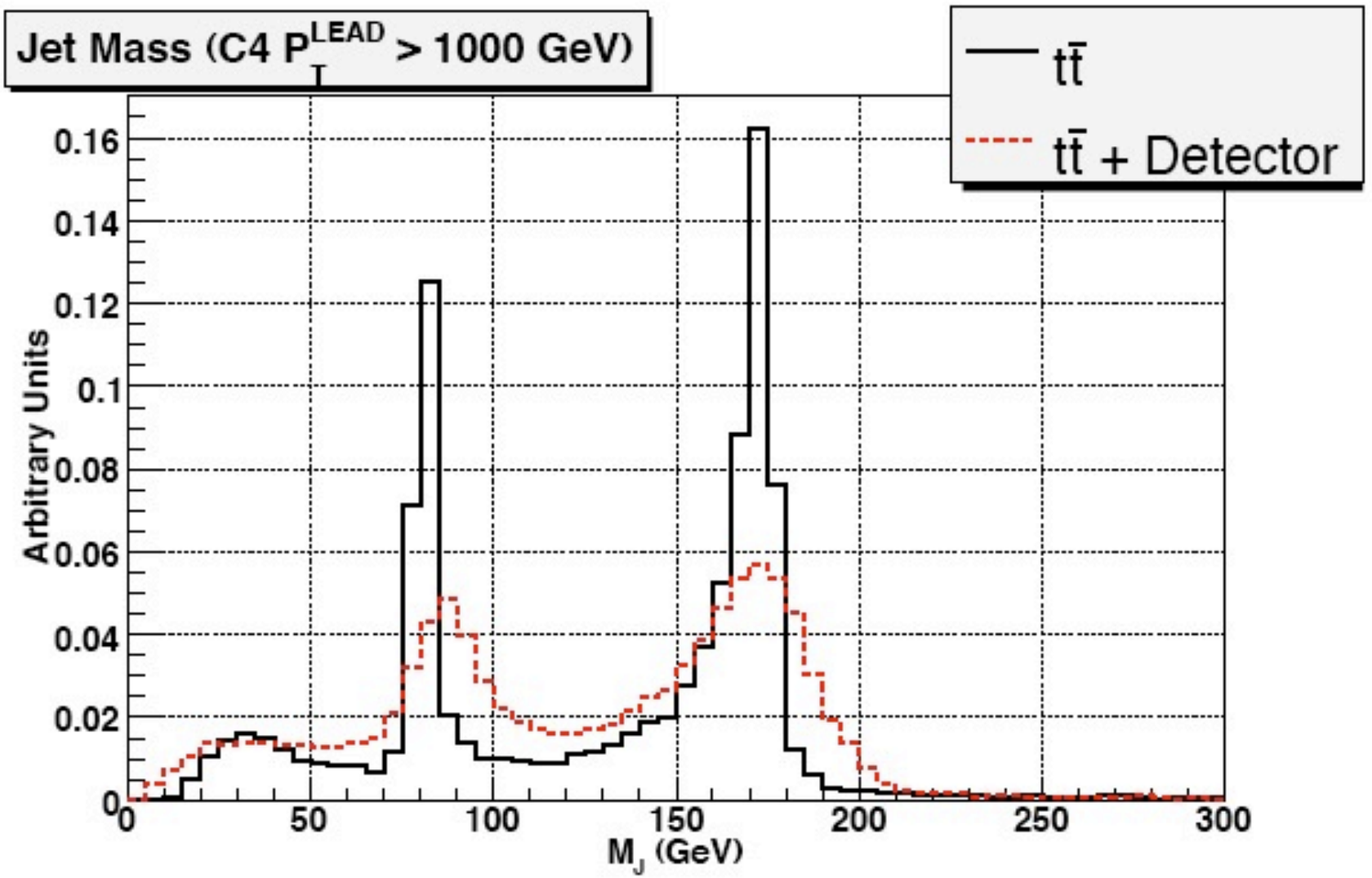

QCD cone jet mass distribution

Boosted QCD Jet via factorization:

$$\frac{d\sigma^i}{dm_J} = J^i\left(m_J, p_T^{min}, R^2\right)\sigma^i\left(p_T^{min}\right)$$

$$i = Q, G$$

$$\int dm_J\, J^i = 1$$

Full expression:

$$\frac{d\sigma_{H_A H_B \to J_1 J_2}}{dm_{J_1}^2 dm_{J_2}^2 d\eta} = \sum_{abcd}\int dx_a\, dx_b\, \phi_a(x_a, p_T)\, \phi_b(x_b, p_T)\frac{d\hat{\sigma}_{ab\to cd}}{dp_T d\eta}(x_a, x_b, \eta, p_T)$$

$$S\left(m_{J_1}^2, m_{J_2}^2, \eta, p_T, R^2\right)\; J_1^{(c)}(m_{J_1}^2, \eta, p_T, R^2) J_2^{(d)}(m_{J_2}^2, \eta, p_T, R^2)$$

QCD cone jet mass distribution

Boosted QCD Jet via factorization:

$$\frac{d\sigma^i}{dm_J} = J^i\left(m_J, p_T^{min}, R^2\right)\sigma^i\left(p_T^{min}\right)$$

$$\int dm_J\, J^i = 1 \qquad i = Q, G$$

For large jet mass & small R,
no big logs =>
J^i can be calculated via
perturbative QCD!

Full expression:

$$\frac{d\sigma_{H_A H_B \to J_1 J_2}}{dm_{J_1}^2 dm_{J_2}^2 d\eta} = \sum_{abcd}\int dx_a\, dx_b\, \phi_a(x_a, p_T)\,\phi_b(x_b, p_T)\frac{d\hat{\sigma}_{ab\to cd}}{dp_T d\eta}(x_a, x_b, \eta, p_T)$$

$$S\left(m_{J_1}^2, m_{J_2}^2, \eta, p_T, R^2\right)\; J_1^{(c)}(m_{J_1}^2, \eta, p_T, R^2) J_2^{(d)}(m_{J_2}^2, \eta, p_T, R^2)$$

QCD Jet mass distribution, Q+G

Main idea: calculating mass due to two-body QCD bremsstrahlung:

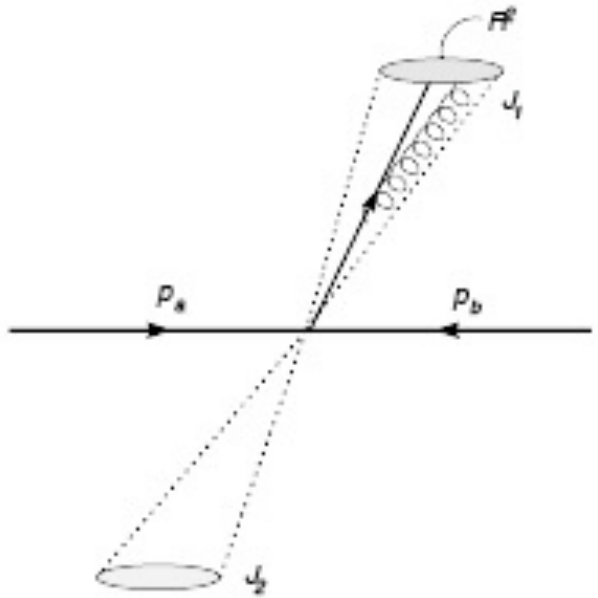

QCD Jet mass distribution, Q+G

Main idea: calculating mass due to two-body QCD bremsstrahlung:

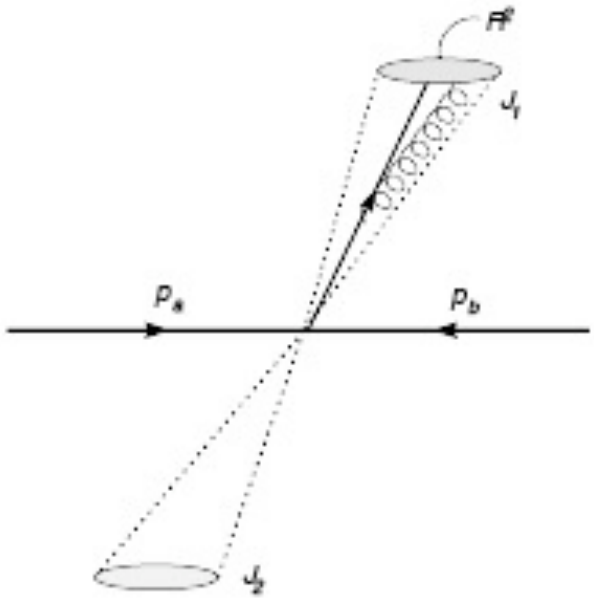

$$J^{(eik),c}(m_J, p_T, R) \simeq \alpha_S(p_T) \frac{4 C_c}{\pi m_J} \log\left(\frac{R\, p_T}{m_J}\right)$$

$C_F = 4/3$ for quarks, $C_A = 3$ for gluons.

QCD Jet mass distribution, Q+G

$$J^{(eik),c}(m_J, p_T, R) \simeq \alpha_S(p_T) \frac{4\,C_c}{\pi m_J} \log\left(\frac{R\,p_T}{m_J}\right)$$

$C_F = 4/3$ for quarks, $C_A = 3$ for gluons.

Data is admixture of the two, should be bounded by them:

$$\frac{d\sigma_{pred}(R)}{dp_T dm_J}_{\ upper\ bound} = J^g(m_J, p_T, R) \sum_c \left(\frac{d\sigma^c(R)}{dp_T}\right)_{\rm MC},$$

$$\frac{d\sigma_{pred}(R)}{dp_T dm_J}_{\ lower\ bound} = J^q(m_J, p_T, R) \sum_c \left(\frac{d\sigma^c(R)}{dp_T}\right)_{\rm MC},$$

Jet mass distribution, theory vs. MC

Sherpa, jet function convolved above $p_T^{\min}$

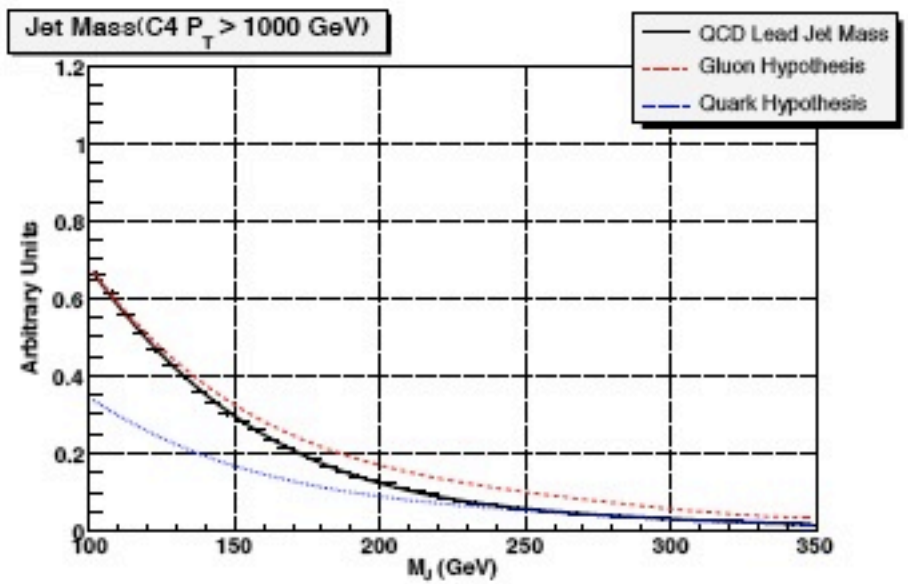

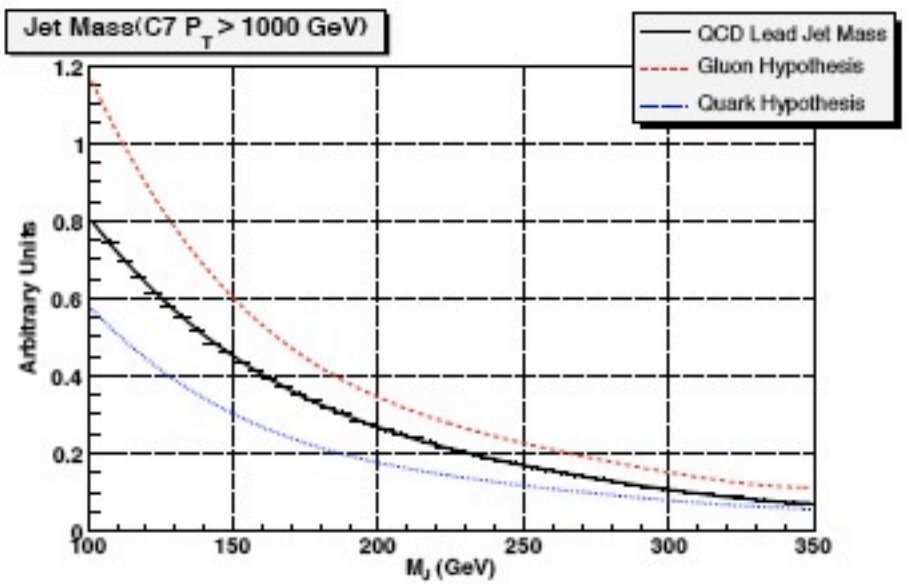

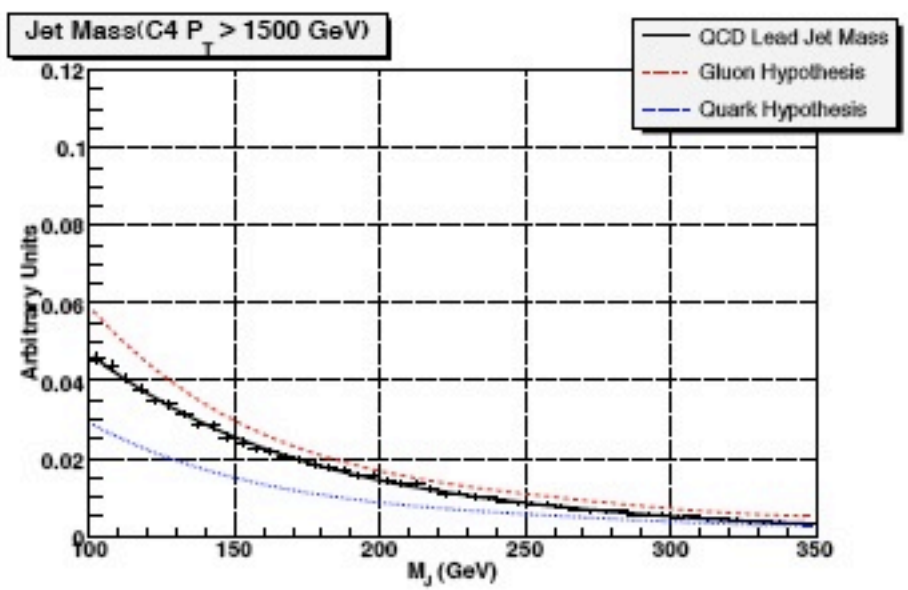

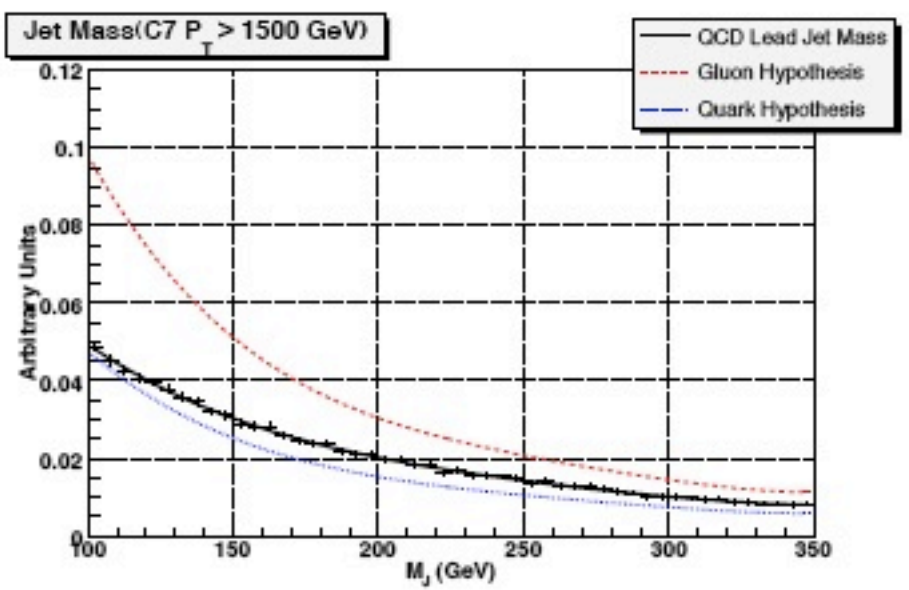

Ex.: SM $t\bar{t}$ vs. di-jet

(fully collimated region)

Ex.: SM $t\bar{t}$ vs. di-jet

(fully collimated region)

SM ttbar vs. di-jet naive mass tagging

Truth-level (no detector effects) results for double-tag jet mass method using, reflecting 100 fb^{-1} of integrated luminosity.

p_T^{lead} cut	Cone size	$t\bar{t}$ (S)	Background (B)	S/B
1000 GeV	C4	3430	13505	0.254
1000 GeV	C7	6302	36765	0.171
1500 GeV	C4	403	1874	0.215
1500 GeV	C7	458	2724	0.168

Naive (truth) rejection power $R = \frac{\epsilon^S}{\epsilon^B} = 20$

Naively 5σ with 2-3 fb^{-1}

Detector effects further reduce it by factor of few $\Rightarrow$ 10's of fb^{-1}.

SM ttbar vs. di-jet naive mass tagging

Truth-level (no detector effects) results for double-tag jet mass method using, reflecting 100 fb^{-1} of integrated luminosity.

p_T^{lead} cut	Cone size	$t\bar{t}$ (S)	Background (B)	S/B
1000 GeV	C4	3430	13505	0.254
1000 GeV	C7	6302	36765	0.171
1500 GeV	C4	403	1874	0.215
1500 GeV	C7	458	2724	0.168

Naive (truth) rejection power $R = \frac{\epsilon^S}{\epsilon^B} = 20$

Naively 5σ with 2-3 fb^{-1}

Detector effects further reduce it by factor of few $\Rightarrow$ 10's of fb^{-1}.

looks hard  even with b-taggs!

SM ttbar vs. di-jet naive mass tagging

Truth-level (no detector effects) results for double-tag jet mass method using, reflecting 100 fb^{-1} of integrated luminosity.

p_T^{lead} cut	Cone size	$t\bar{t}$ (S)	Background (B)	S/B
1000 GeV	C4	3430	13505	0.254
1000 GeV	C7	6302	36765	0.171
1500 GeV	C4	403	1874	0.215
1500 GeV	C7	458	2724	0.168

Naive (truth) rejection power $R = \frac{\epsilon^S}{\epsilon^B} = 20$

Naively 5σ with 2-3 fb^{-1}

Detector effects further reduce it by factor of few $\Rightarrow$ 10's of fb^{-1}.

looks hard  even with b-taggs!

Remove background via side band analysis

Can use our understanding of background shapes to fit for the data.

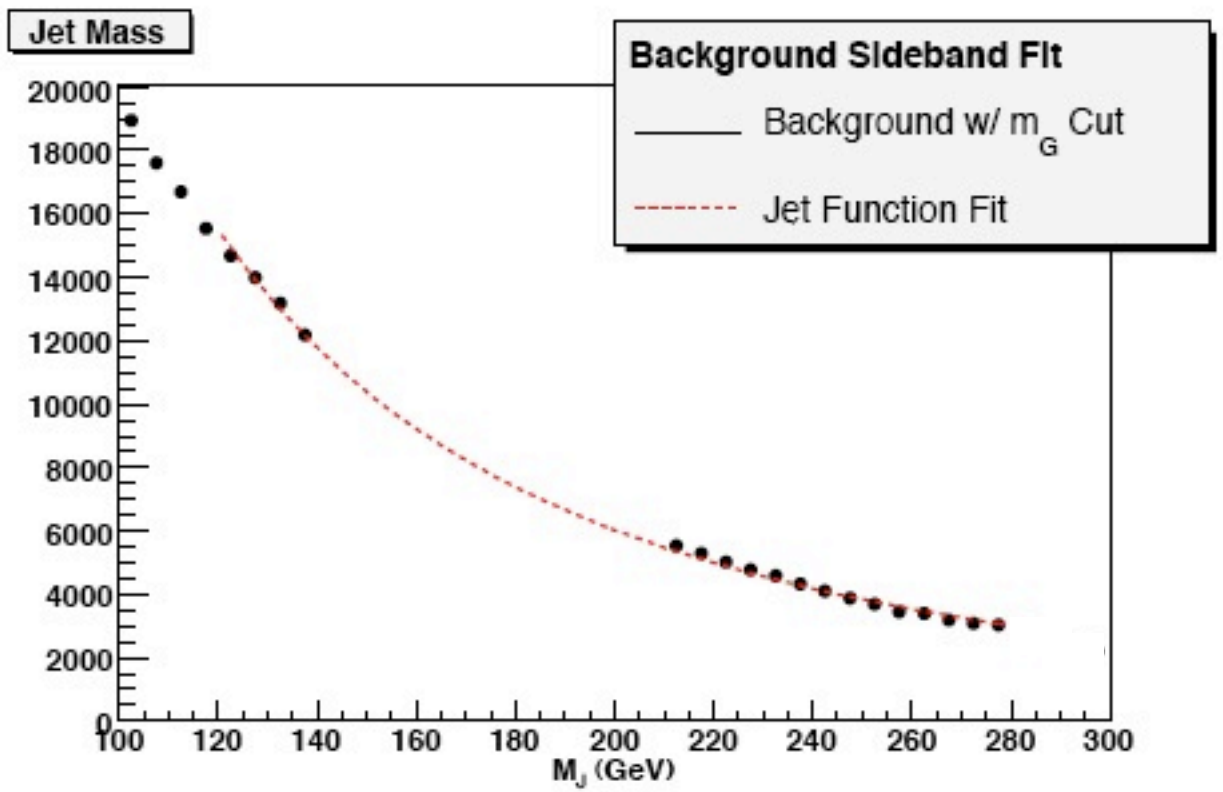

A typical example of fitting jet functions to the jet mass distribution in the sideband regions ($120\,\text{GeV} \leq m_J \leq 140\,\text{GeV}$) $\cup$ ($210\,\text{GeV} < m_J < 280\,\text{GeV}$). This plot corresponds to a single-tag analysis with C7 jets with $p_T \geq 1000\,\text{GeV}$.

Remove background via side band analysis

Can use our understanding of background shapes to fit for the data. (only 4 input parameters, 18 bins)

$$F(m_J) = N_B \times b(m_J) + N_S \times s(m_J),$$

$$b(m_J) \propto \beta(m_J) \times J^Q\left(m_J; p_T^{min}, R\right) + (1 - \beta(m_J)) \times J^G\left(m_J; p_T^{min}, R\right),$$

where $\beta(m_J)$ is a linear polynomial $\left(\beta_0 + \beta_1 \frac{m_J}{p_T^{min} R}\right)$.

Significance: $n_\sigma = \sqrt{2\left(\log \mathcal{L} - \log \mathcal{L}_0\right)},$

$$\mathcal{L} = \prod_{k=1}^{N_{\text{BINS}}} \frac{\exp\left(-F(m_k)\right) \times \left[F(m_k)\right]^{N_k}}{N_k!}.$$

Remove background via side band analysis

Can use our understanding of background shapes to fit for the data. (only 4 input parameters, 18 bins)

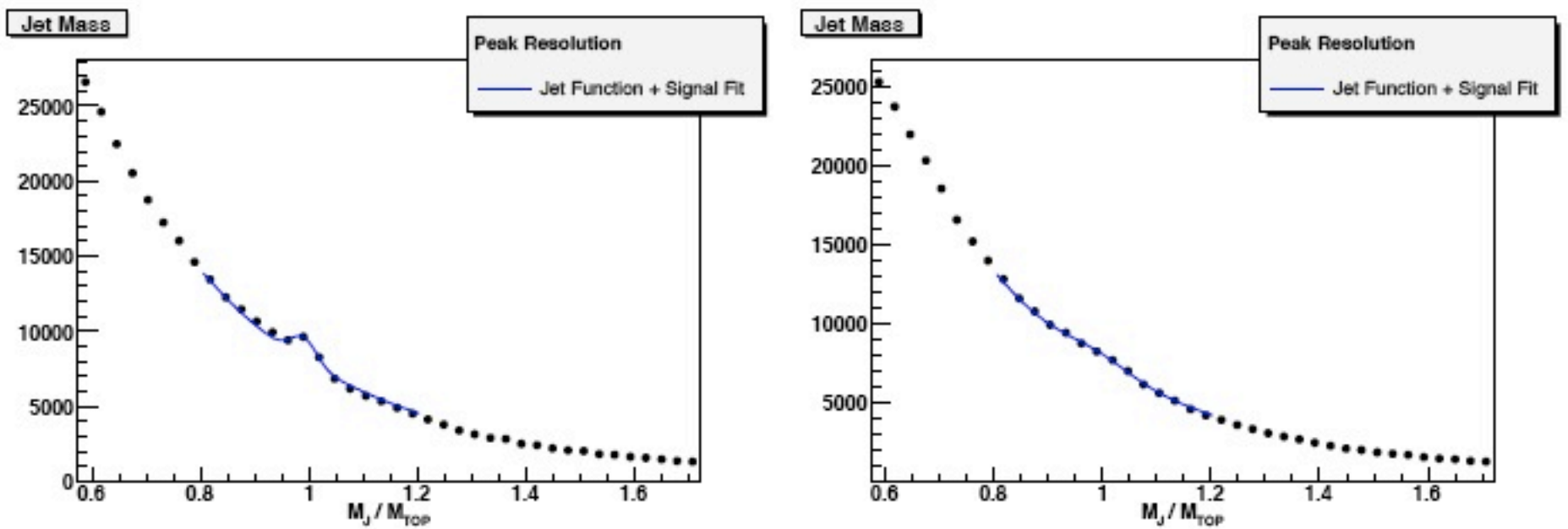

The results of fitting jet functions + signal shape to the jet mass distribution in the top mass window. The plot on the left corresponds to a truth-jet analysis. The plot on the right depicts the effects of detector smearing. The statistics reflect 100 fb^{-1} of integrated luminosity.

Summary, mass tagging

Resolve signal from dijet background:

$$p_T^{min} \sim 1 \text{ TeV and } 25\,\text{fb}^{-1}$$

$$p_T^{min} \sim 1.5\,\text{TeV with } 100\ \text{fb}^{-1}$$

without jet substructure or b-tagging

Note that if S/B is enhanced,
as in RS or other NP models reach is better.

Jet sub-structure

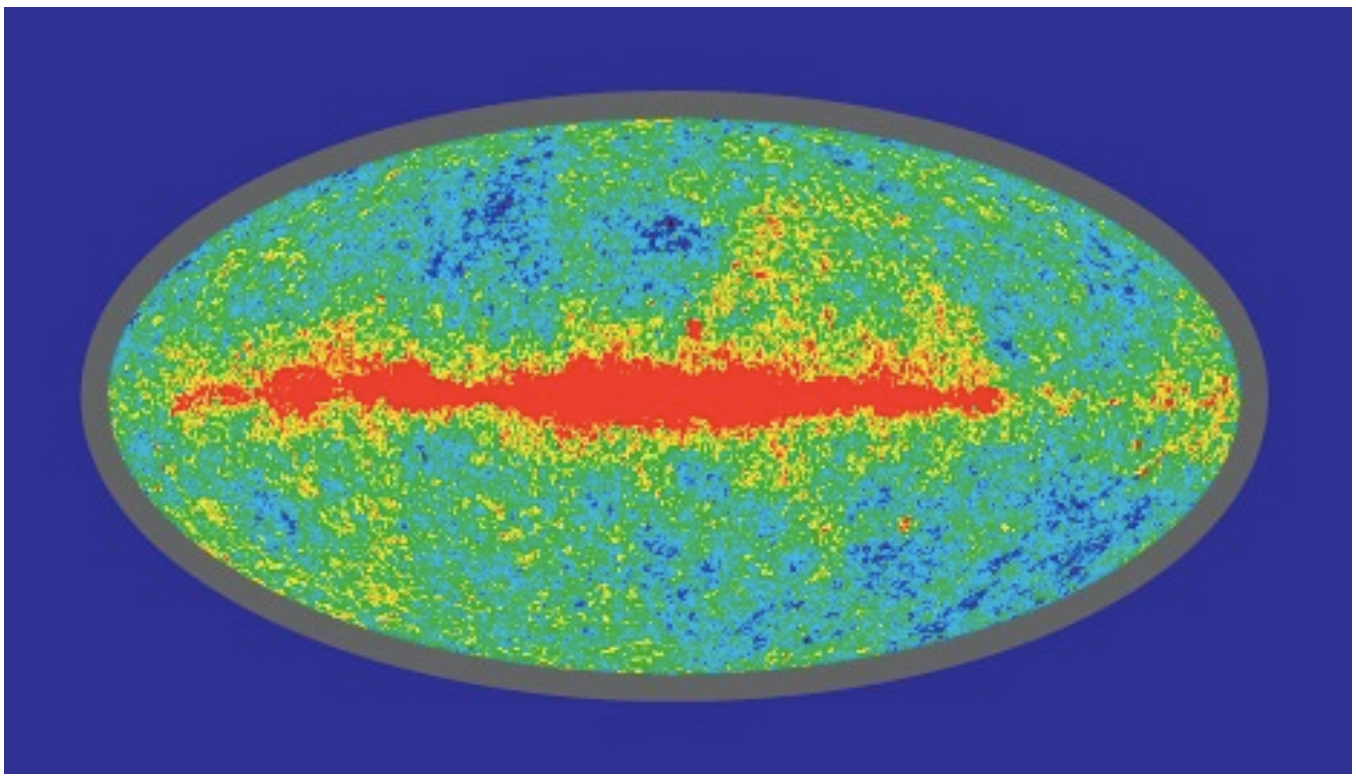

Almeida, Lee, GP, Sterman, Sung & Virzi; Brooijmans; Butterworth, et. al.; Thaler & Wang; Conway; Vos; Kaplan, Rehermann, Schwartz & Tweedie.

IRC-safe jet-shapes which know top from QCD jets?

- Successes in high jet mass => jet function is well described by single gluon radiation.
- As a warmup consider angularity (2-body final state):

Berger, K´ucs and Sterman (03)

Angularities on a cone:

$$\tilde{\tau}_a(R, p_T) = \frac{1}{m_J} \sum_{i \in jet} \omega_i \sin^a\left(\frac{\pi\theta_i}{2R}\right) \left[1 - \cos\left(\frac{\pi\theta_i}{2R}\right)\right]^{1-a}$$

Almeida, Lee, GP, Sterman, Sung, & Virzi.

- Can evaluate distribution, fixing the mass => simplification.

2-body jet's kinematics, $Z/W/h$

$$P^x(\theta_s) = (dJ^x/d\theta_s)/J^x \Rightarrow P^x(\tilde{\tau}_a)\,; \qquad R(\tilde{\tau}_a) = \frac{P^{\rm sig}(\tilde{\tau}_a)}{P^{\rm QCD}(\tilde{\tau}_a)}$$

2-body jet's kinematics, $Z/W/h$

$$P^x(\theta_s) = (dJ^x/d\theta_s)/J^x \Rightarrow P^x(\tilde{\tau}_a)\,; \qquad R(\tilde{\tau}_a) = \frac{P^{\rm sig}(\tilde{\tau}_a)}{P^{\rm QCD}(\tilde{\tau}_a)}$$

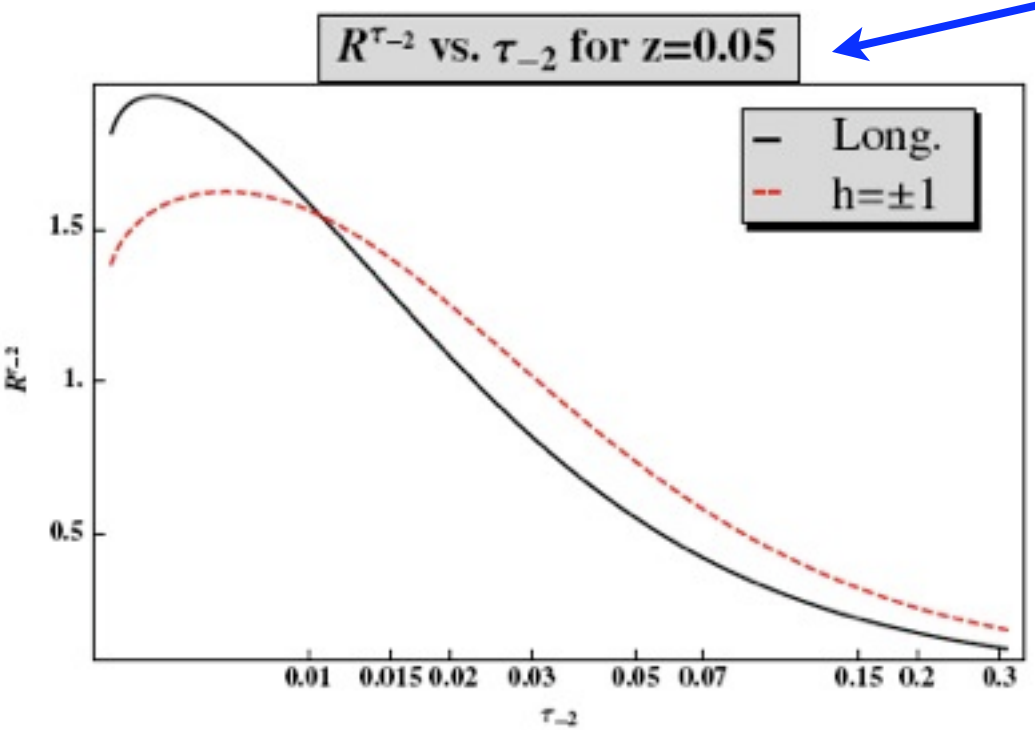

FIG. 3 (color online). The ratio between the signal and background probabilities to have jet angularity $\tilde{\tau}_{-2}$, $R^{\tilde{\tau}_{-2}}$.

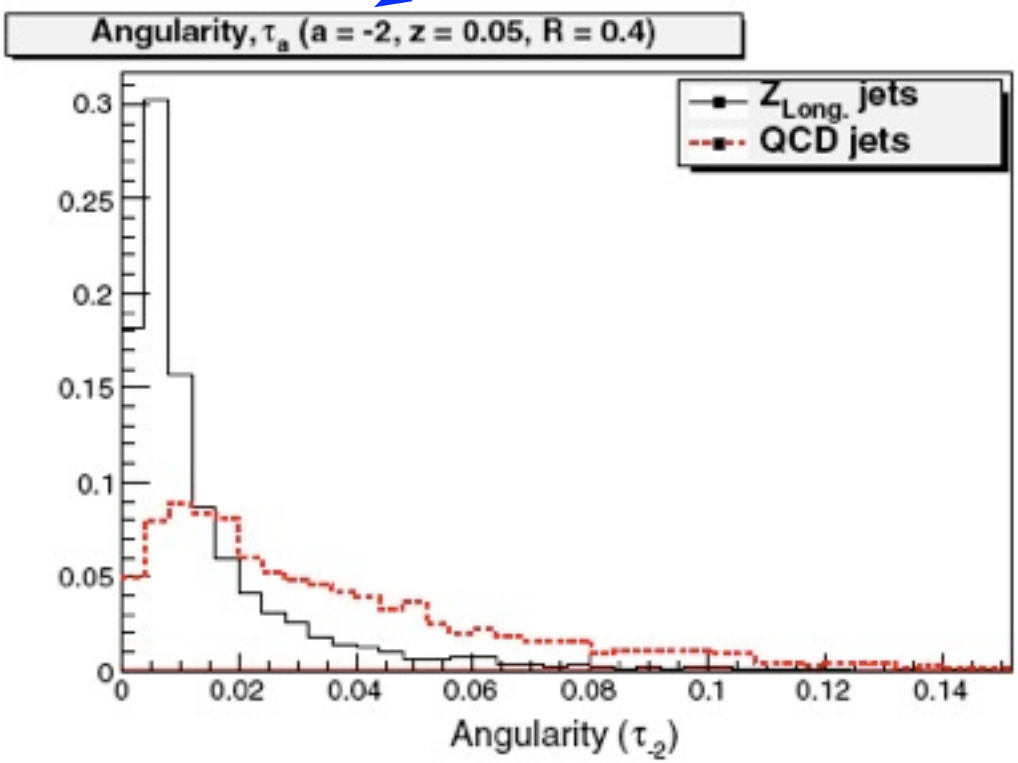

FIG. 4 (color online). The angularity distribution for QCD (red-dashed curve) and longitudinal Z (black-solid curve) jets obtained from MADGRAPH. Both distributions are normalized to the same area.

$$(z = m_J/p_T)$$

2-body jet's kinematics, $Z/W/h$

$$P^x(\theta_s) = (dJ^x/d\theta_s)/J^x \Rightarrow P^x(\tilde{\tau}_a)\,; \qquad R(\tilde{\tau}_a) = \frac{P^{\rm sig}(\tilde{\tau}_a)}{P^{\rm QCD}(\tilde{\tau}_a)}$$

Peak => special "democratic" configuration where the two particles have same energy & min' distance from jet axis $\theta_m \approx z$.

$$(z = m_J/p_T)$$

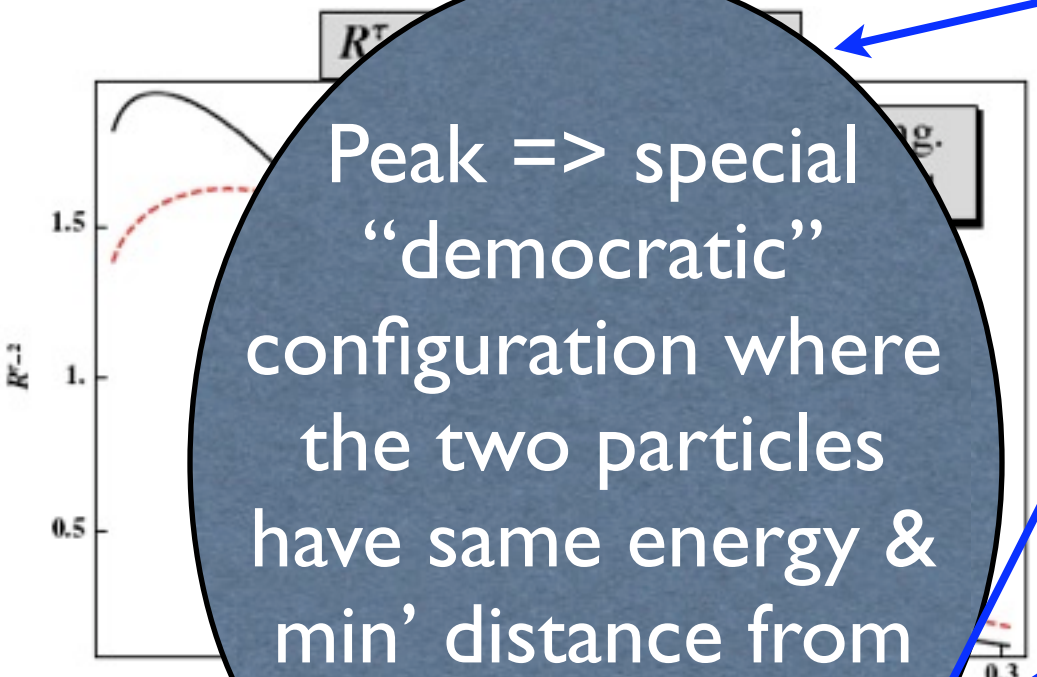

FIG. 3 (color … ground prob… …nd back-

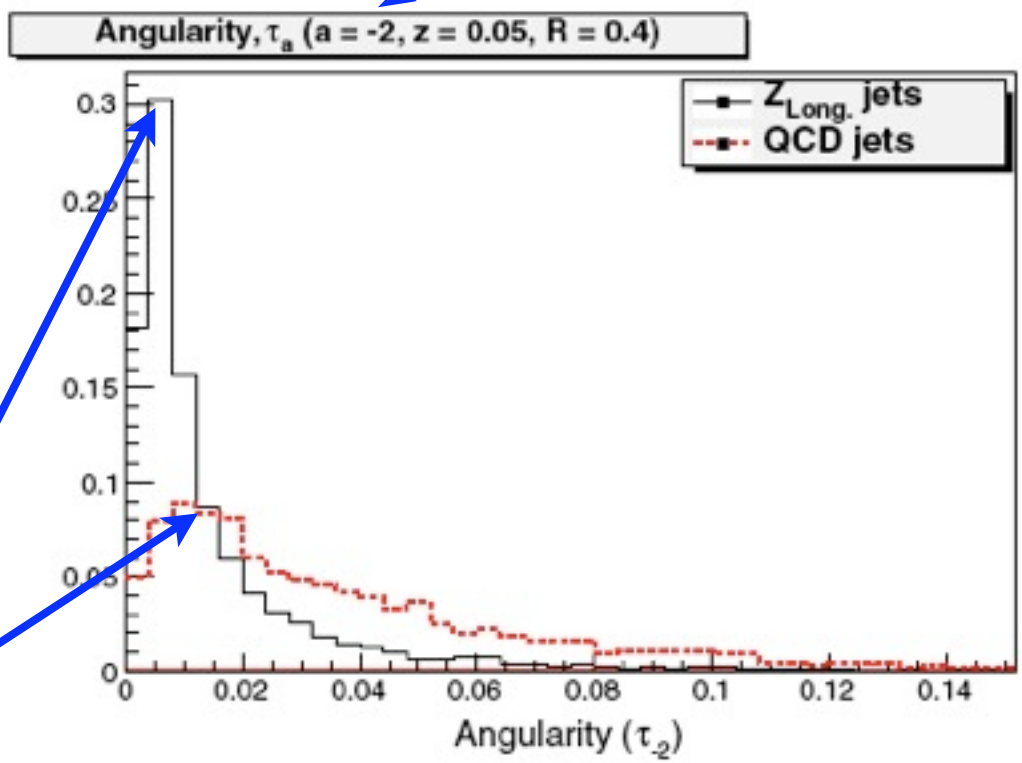

FIG. 4 (color online). The angularity distribution for QCD (red-dashed curve) and longitudinal Z (black-solid curve) jets obtained from MADGRAPH. Both distributions are normalized to the same area.

2-body jet's kinematics, $Z/W/h$

t-jets are essentially different due to the W decay (3 body)

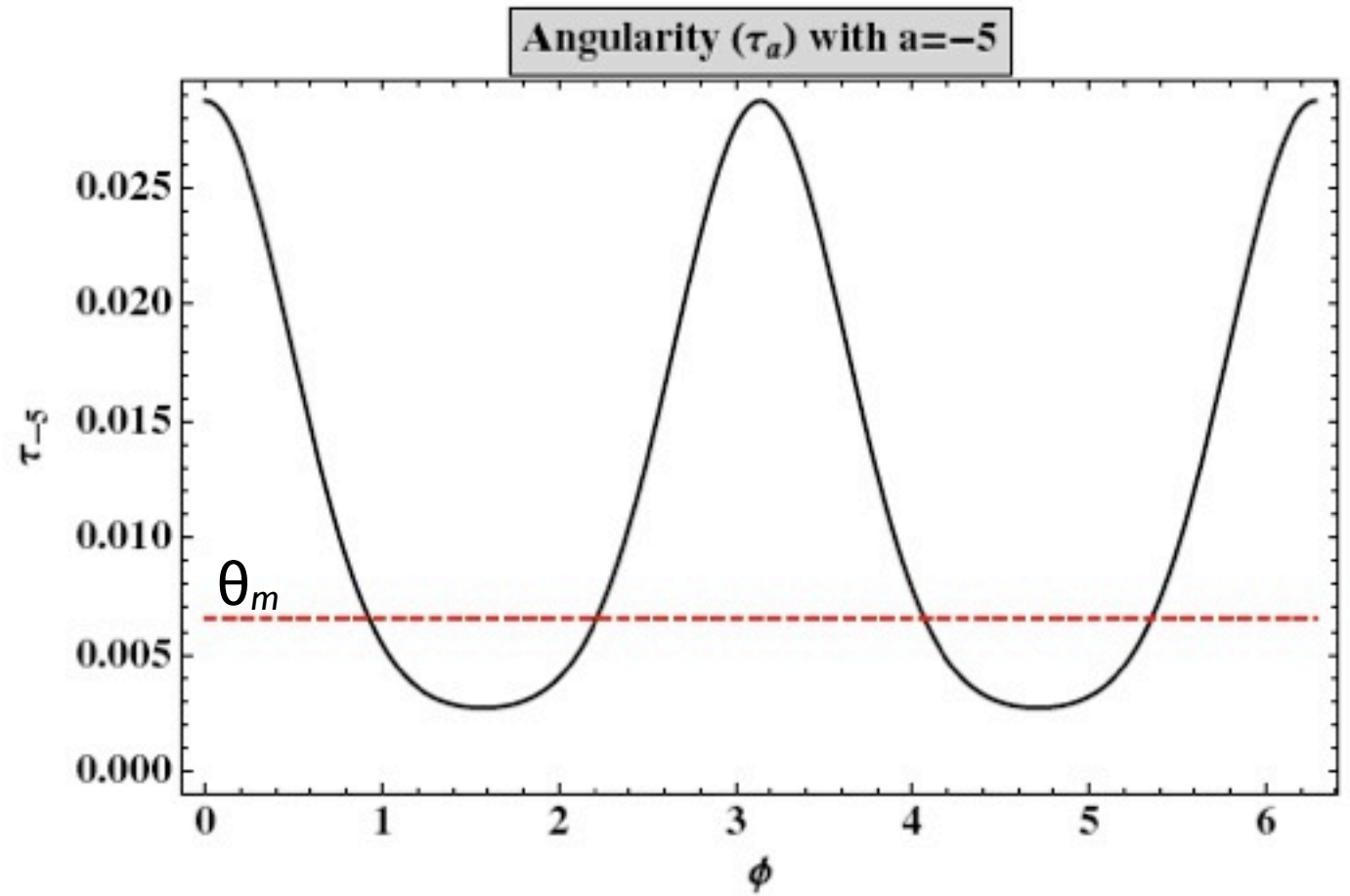

FIG. 3 (color
ground prob

ty distribution for QCD
(black-solid curve) jets
butions are normalized to

$(z =$

FIG. 5 (color online). Angularity, $\tilde{\tau}_{-5}$ as a function of the azimuthal angle of the $W(q\bar{q})$ pair, ϕ_q, for a typical top jet event, compared to the typical case two-body kinematics.

QCD jets vs top jets via planar flow

- QCD jets are democratic & broad, shown both for cone & anti-k_t jets.

SISCone QCD Jet

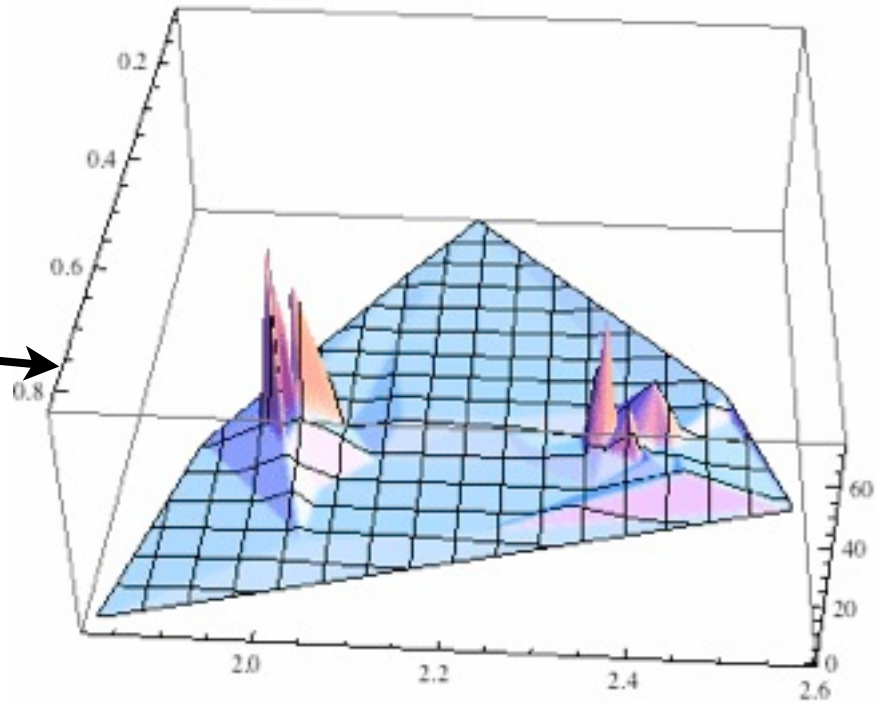

QCD jets vs top jets via planar flow

- QCD jets are democratic & broad, shown both for cone & anti-k_t jets.

SISCone QCD Jet

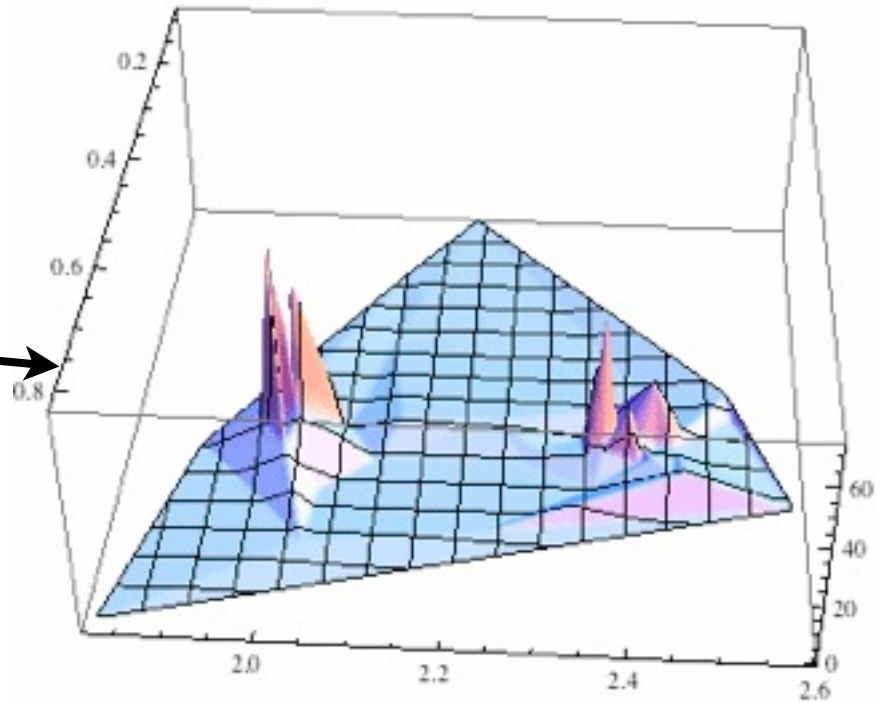

- QCD, top: linear, planar E-deposition in the cone.
- IR-safe E-flow tensor: $I_w^{kl} = \frac{1}{m_J} \sum_i w_i \frac{p_{i,k}}{w_i} \frac{p_{i,l}}{w_i}$
- Planar flow: $Pf = \frac{4 \det(I_w)}{\mathrm{tr}(I_w)^2} = \frac{4\lambda_1 \lambda_2}{(\lambda_1 + \lambda_2)^2}$

Planar flow, QCD vs top jets

Planar flow, QCD vs top jets

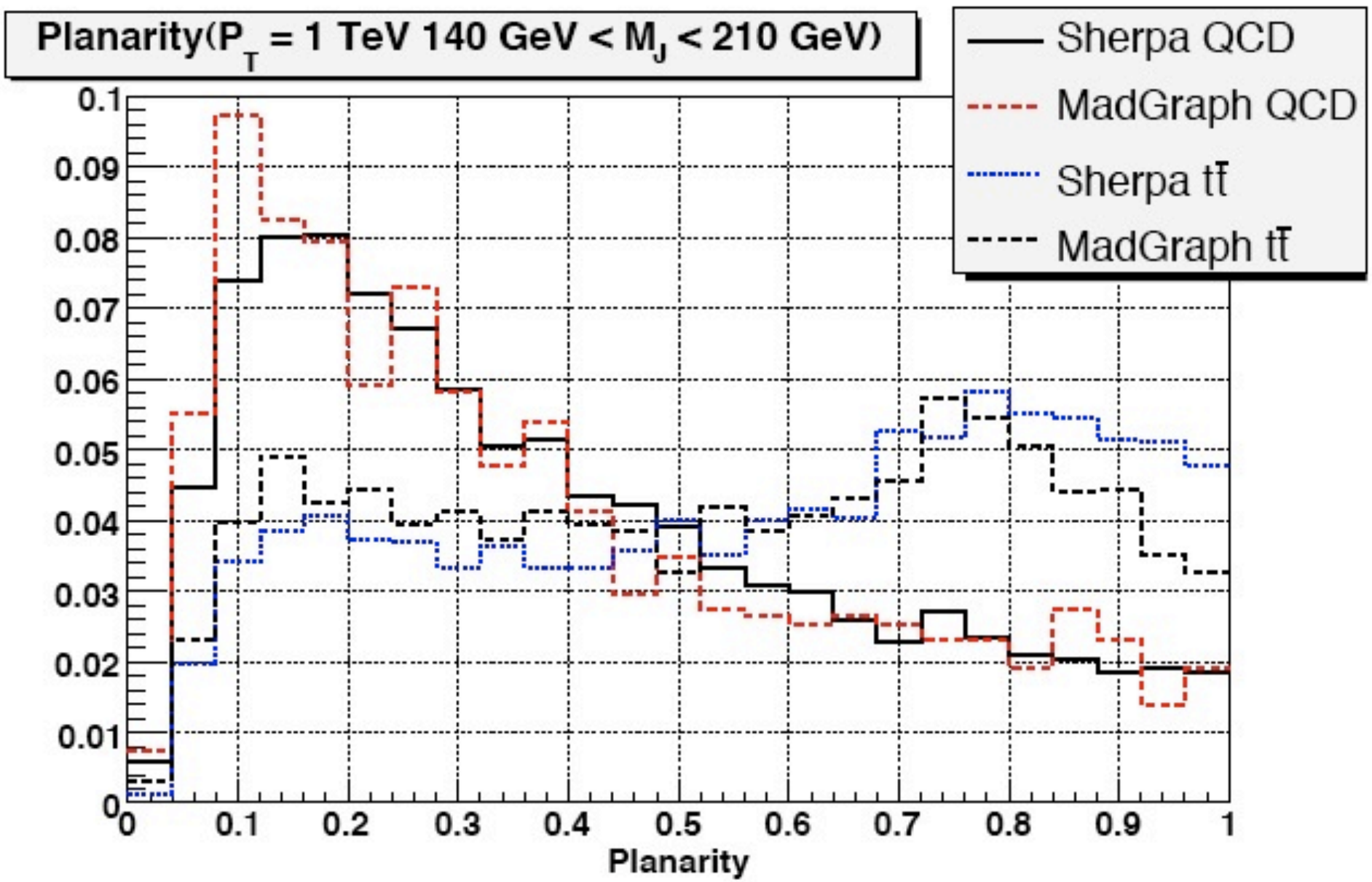

Planar flow, QCD vs top jets

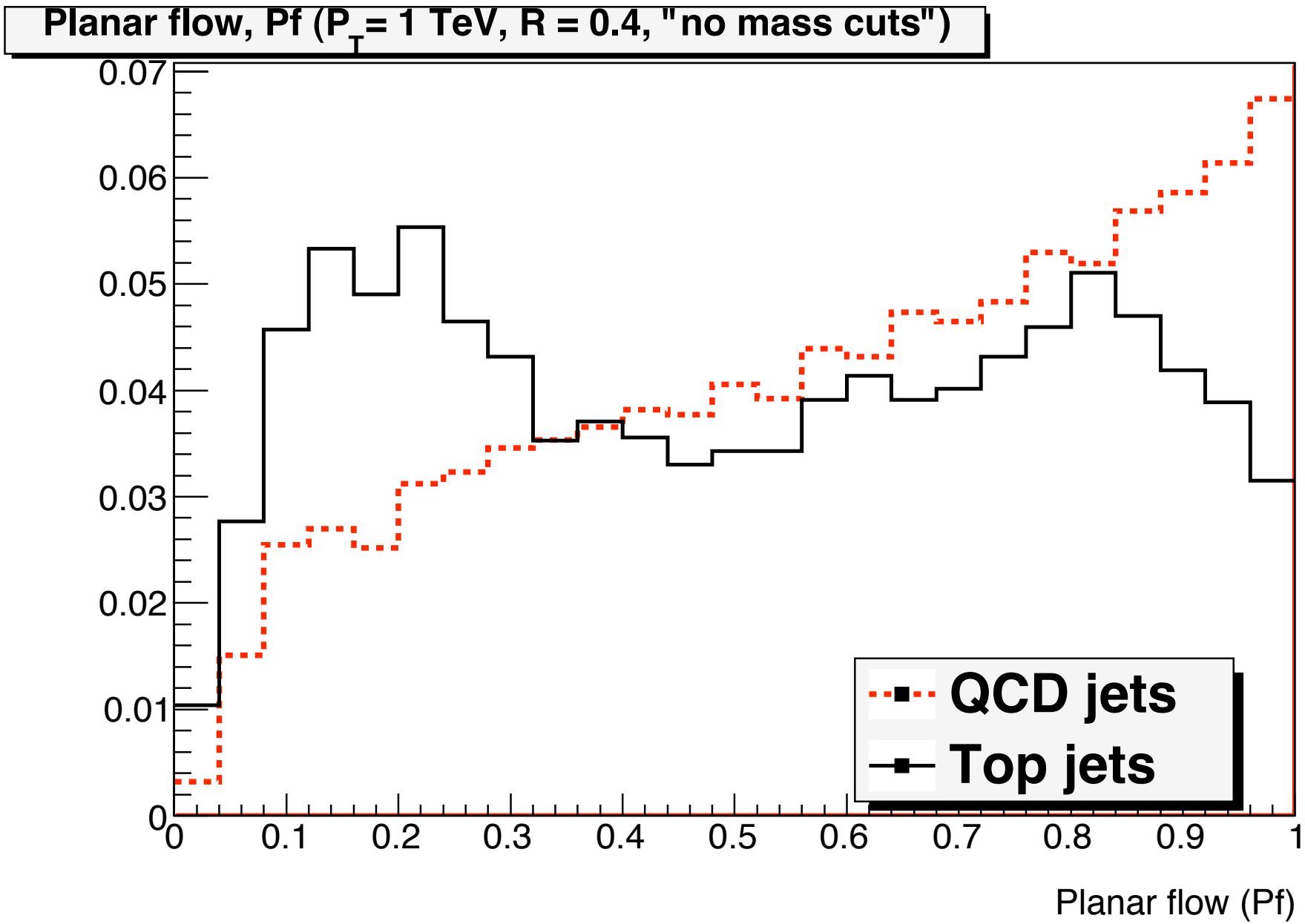

Planar flow, QCD vs top jets

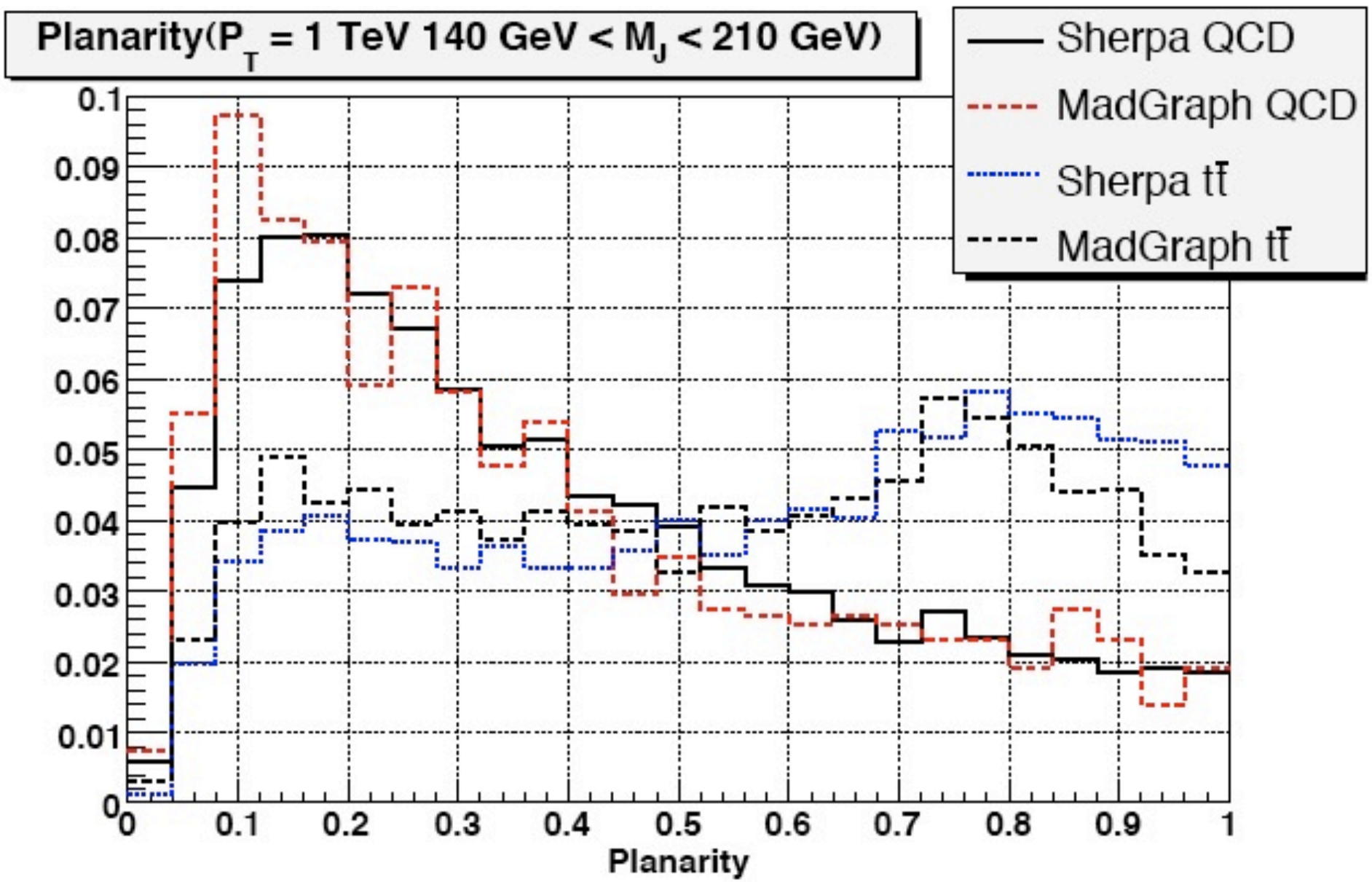

Planar flo CD vs top jets

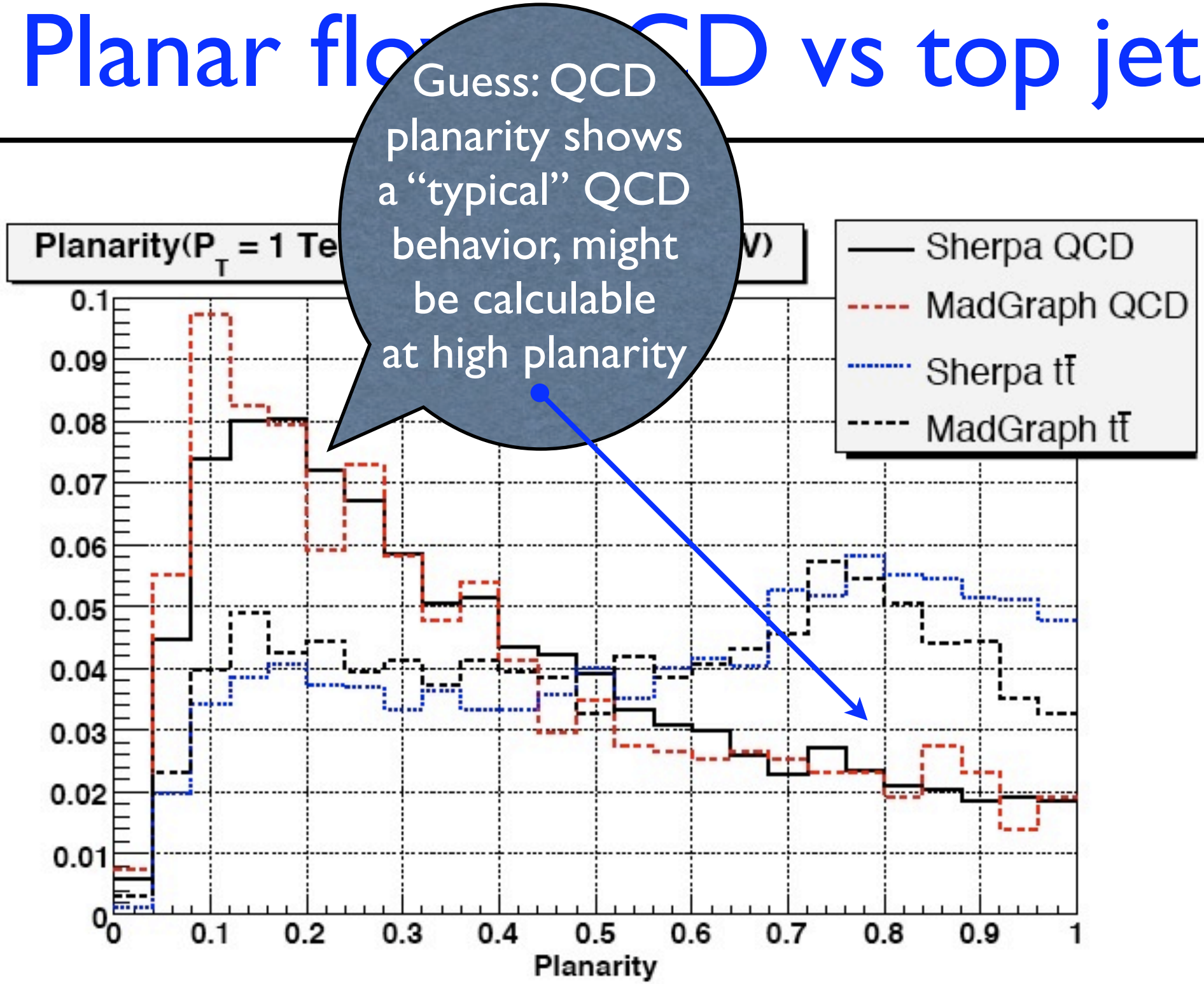

Planar flow, QCD vs top jets

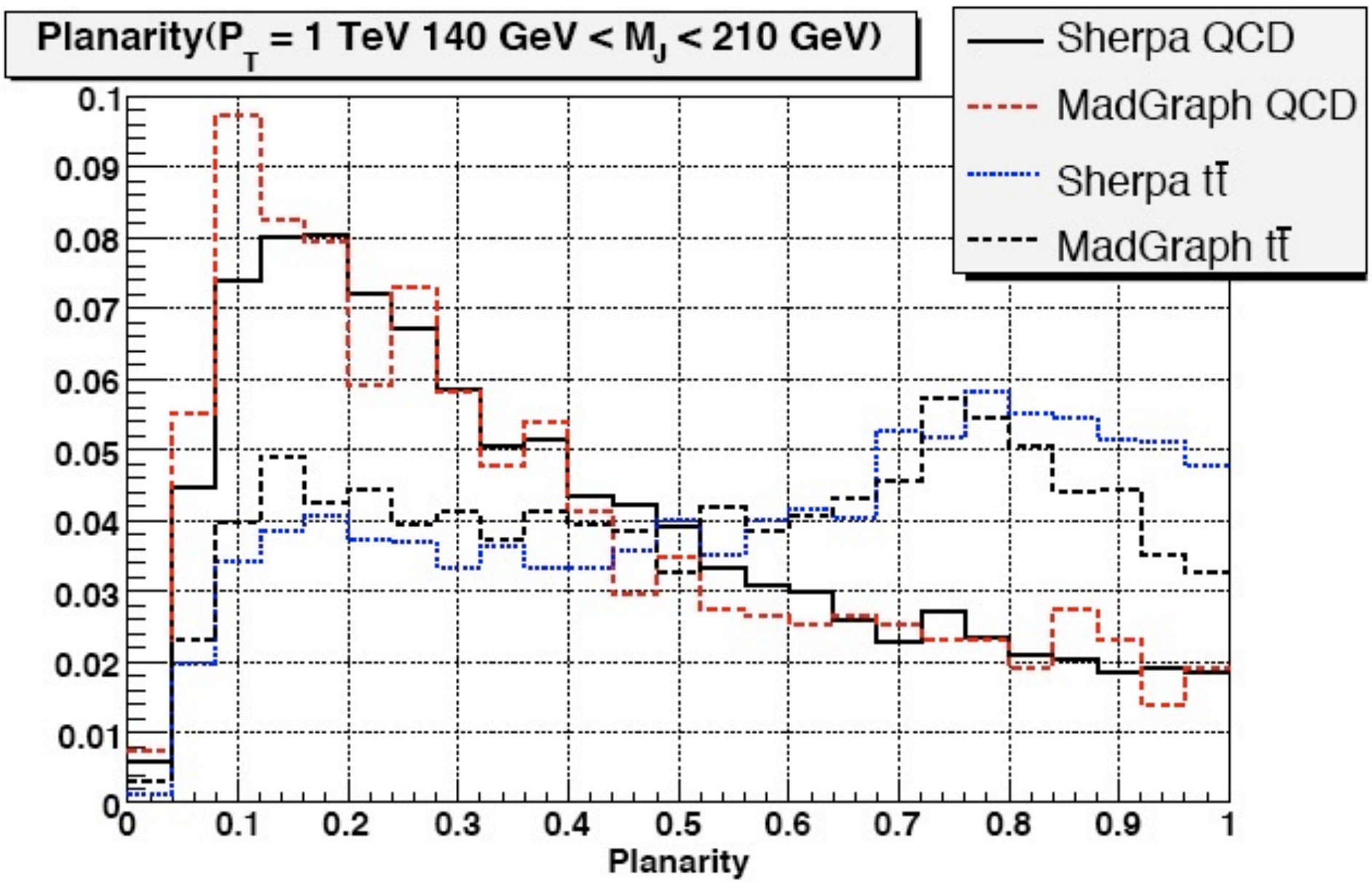

Planar flow, QCD vs top jets

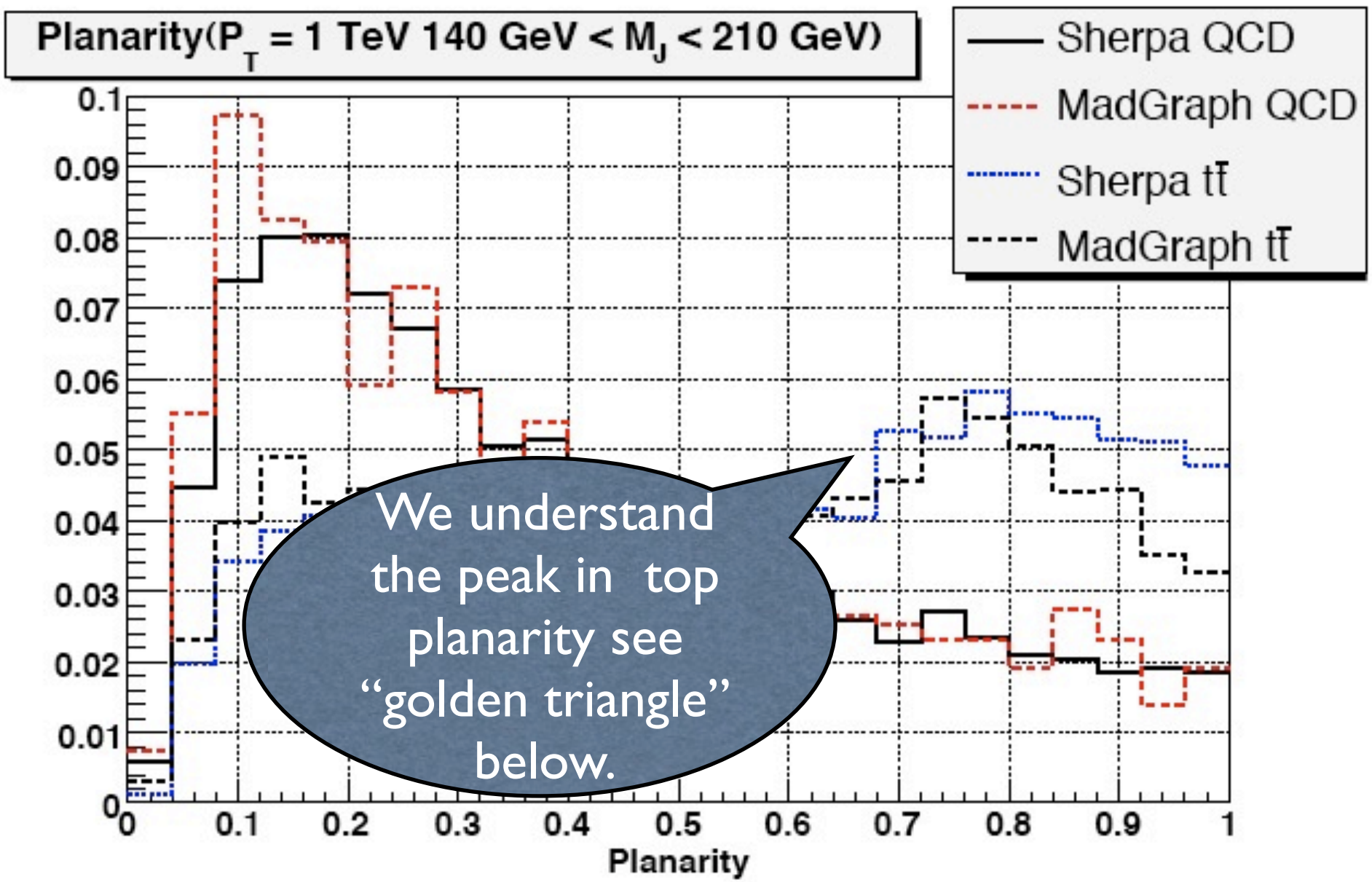

Planar flow, QCD vs top jets

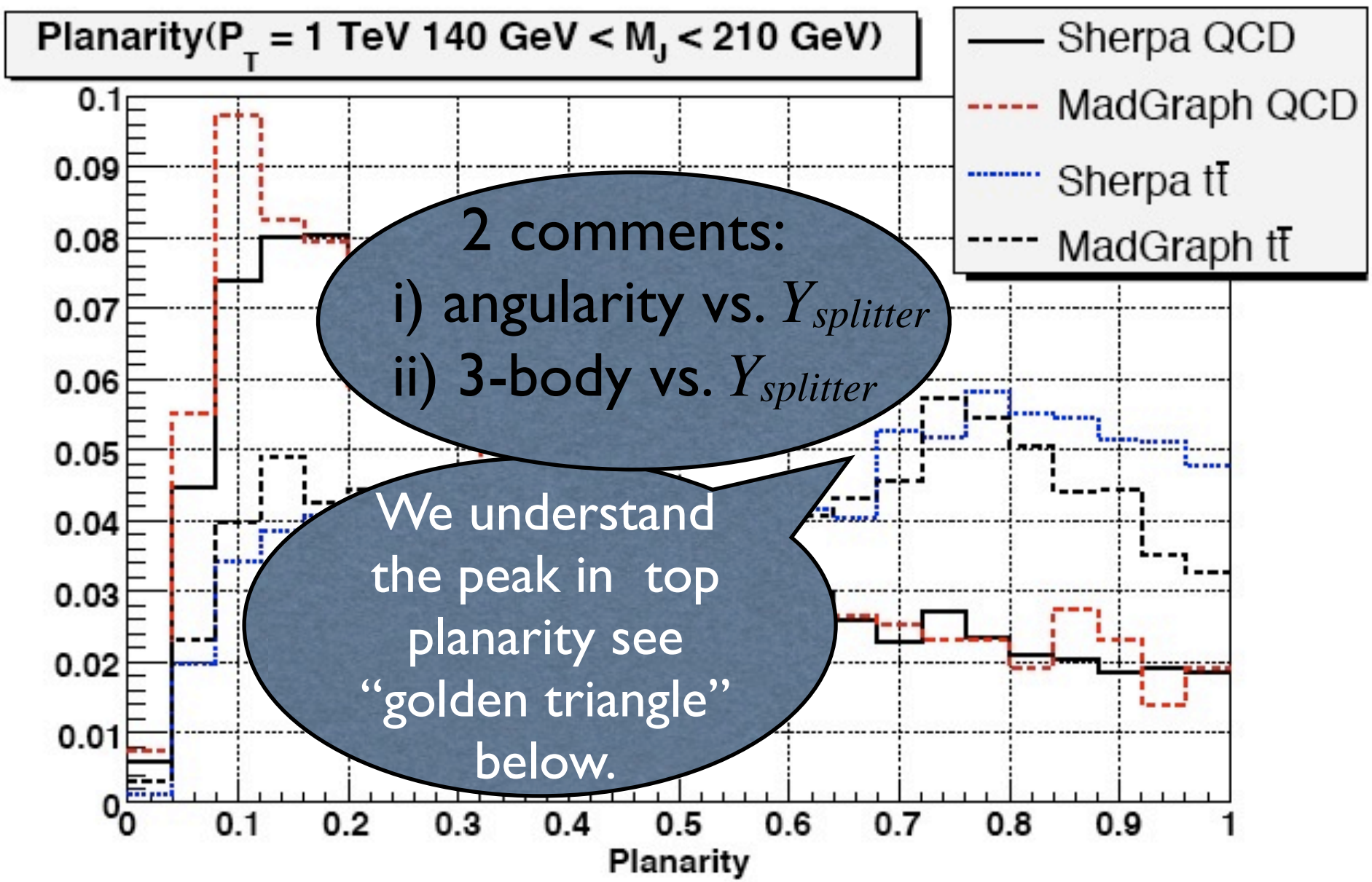

Living of the tails

Lee, GP, Weiler & Zupan.

Many top pairs isn't fully collimated

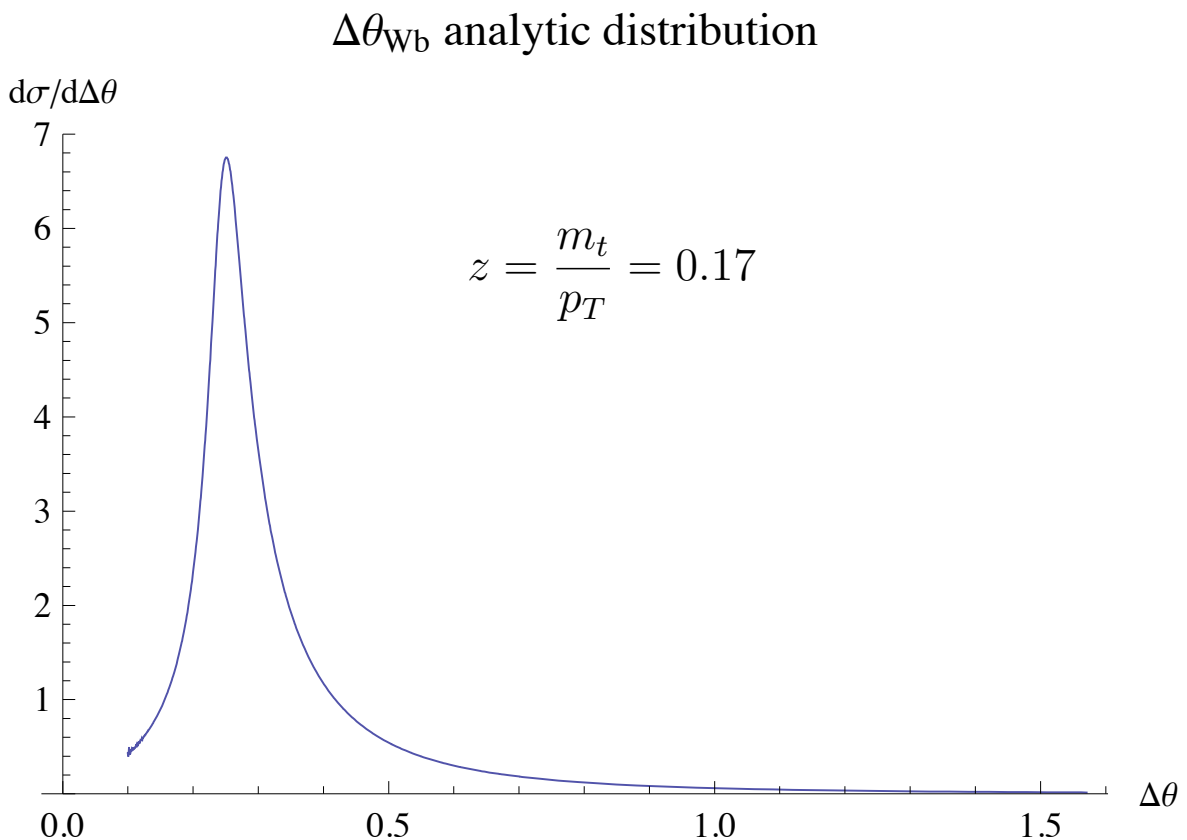

$$R_{\mathrm{col}}^{Wb} \sim 0.8 \Rightarrow \quad \mathrm{non-collimated\ frac} \sim 1 - \left(R_{\mathrm{col}}^{Wb}\right)^2 \sim 0.4!$$

Lee, GP, Weiler & Zupan.

Many top pairs isn't fully collimated

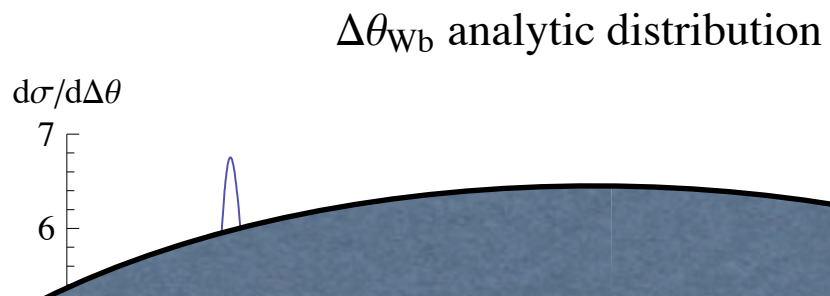

For the non-fully col' use a semi-conventional approach.
Better understood & less challenging for the detector.
Might be used as a control sample

$$R_{\rm col}^{Wb} \sim 0.8 \Rightarrow \quad {\rm non-collimated\ frac} \sim 1 - \left(R_{\rm col}^{Wb}\right)^2 \sim 0.4!$$

Lee, GP, Weiler & Zupan.

An efficient IRC-safe algorithm is constructed, adapted to detector

Lee, GP, Weiler & Zupan.

- Acceptance: events with $p_T > 1000\text{TeV}$ $R < 1$ (SiSCone/KT/Cone)
- Jet finder given $R < 0.4$ (SISCone/anti-K_T/Cone).
- Events are broken into number of jets:
- 1+1: two separated jets have top mass = fully collimated.
- 2+1: requiring mass tagger on one side.
  One the other side requiring $m_j^{1,2} = m_W$ and $m_j^{12} = m_t$.

$$\frac{\epsilon_S^{1+2}}{\epsilon_B^{1+2}} \sim 50,\ 70\,(\text{MG},\ \text{AlpGen})$$

Addition significance is coming from the 1+1 and 2+2 etc ...

An efficient IRC-safe algorithm is constructed, adapted to detector

Lee, GP, Weiler & Zupan.

- Acceptance: events with $p_T > 1000\text{TeV}$ $R < 1$ (SiSCone/KT/Cone)
- Jet finder given $R < 0.4$ (SISCone/anti-K_T/Cone).
- Events are broken into number of jets:
- 1+1: two separated jets have top mass = fully collimated.
- 2+1: requiring mass tagger on one side.
  One the[illegible] $m_j^{12} = m_t$.

b-tagger should be easier since b jet are softer in the 2+1 case.

Addition sig[illegible]2 etc ...

Beyond Planarity, "Probe Function"

- Planarity is a single variable in a 4D 3-body kinematical-variable phase-space => info' is lost.
- Can we be more systematic in our approach?

(Disclaimer: this part is all preliminary, under study.)

$$|t> \;=\; \text{top distribution}$$
$$|g> \;=\; \text{massless QCD distribution}$$

We need a probe distribution, $|f>$, such that

$$R = \left(\frac{<f|t>}{<f|g>}\right) \text{ is maximized.}$$

Guess Probe Function, "Golden Triangle"

- Short cut, using the top dist'?
- Top dist' is still complicated (3D), can we estimate it where it peaks, $\theta_m^{Wb}, \theta_m^{q\bar{q}}$?
- Fix one more (dummy) angle, $\phi^{q\bar{q}}$, to maximize planarity.
- The triangle shape is fixed up to orientation relative to the jet axis, ϕ^{Wb} .

The Golden Triangle

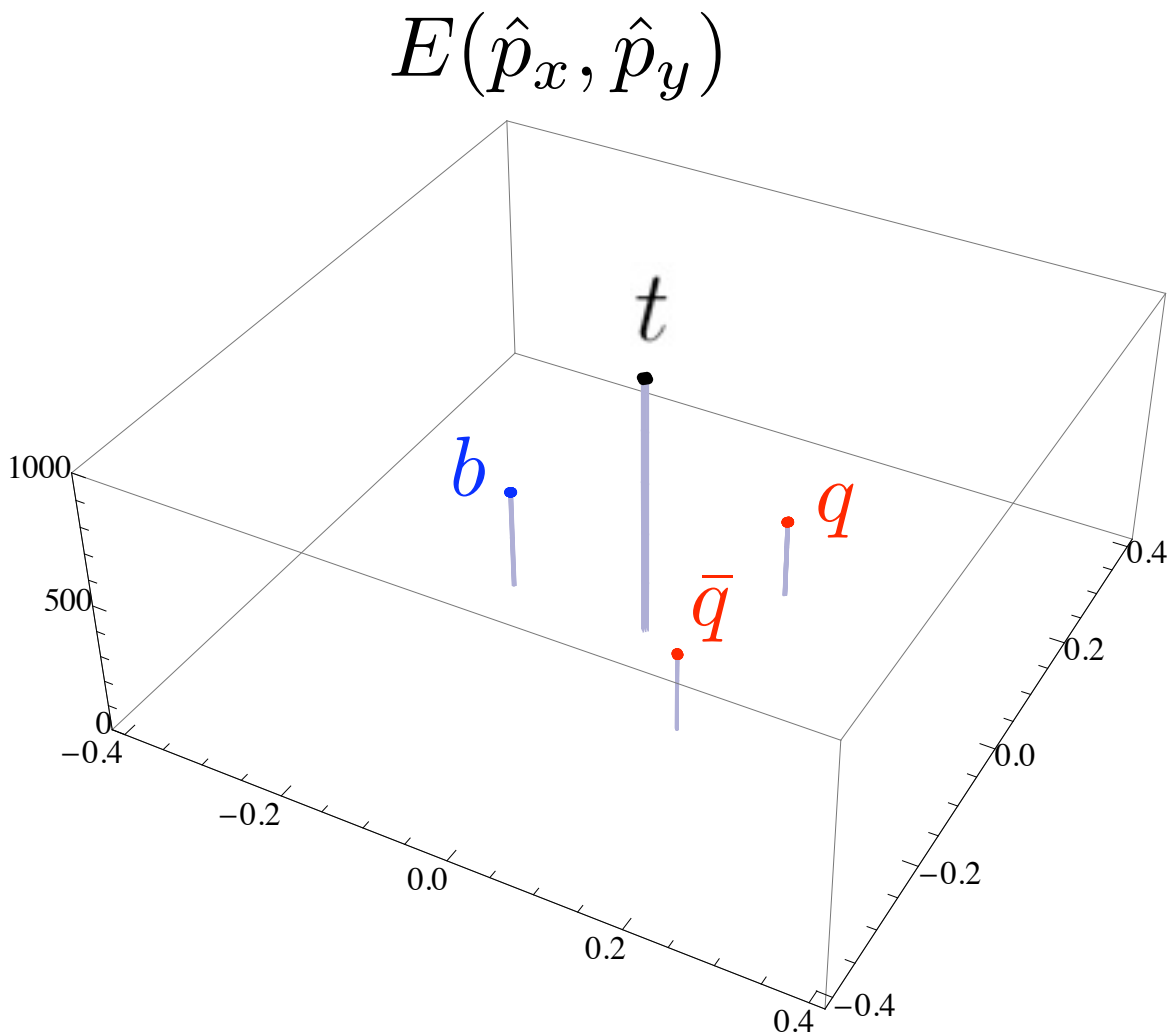

The Golden Triangle

$\theta \sim \frac{m_t}{p_T}$ is the distance from the jet axis;
ϕ is the azimuth angle.

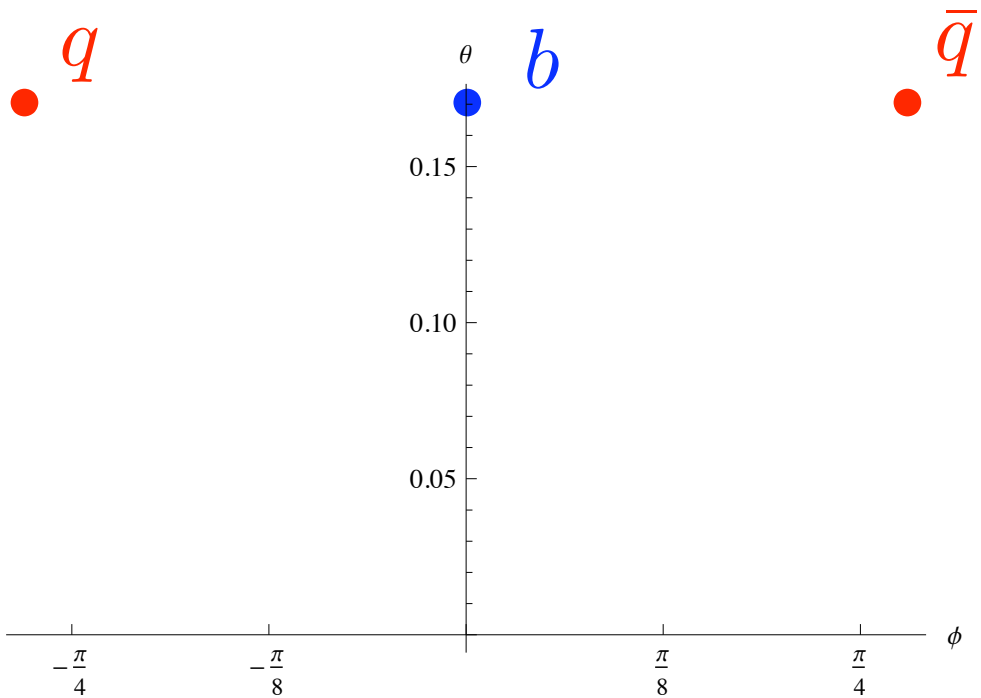

The Golden Triangle & events overlap

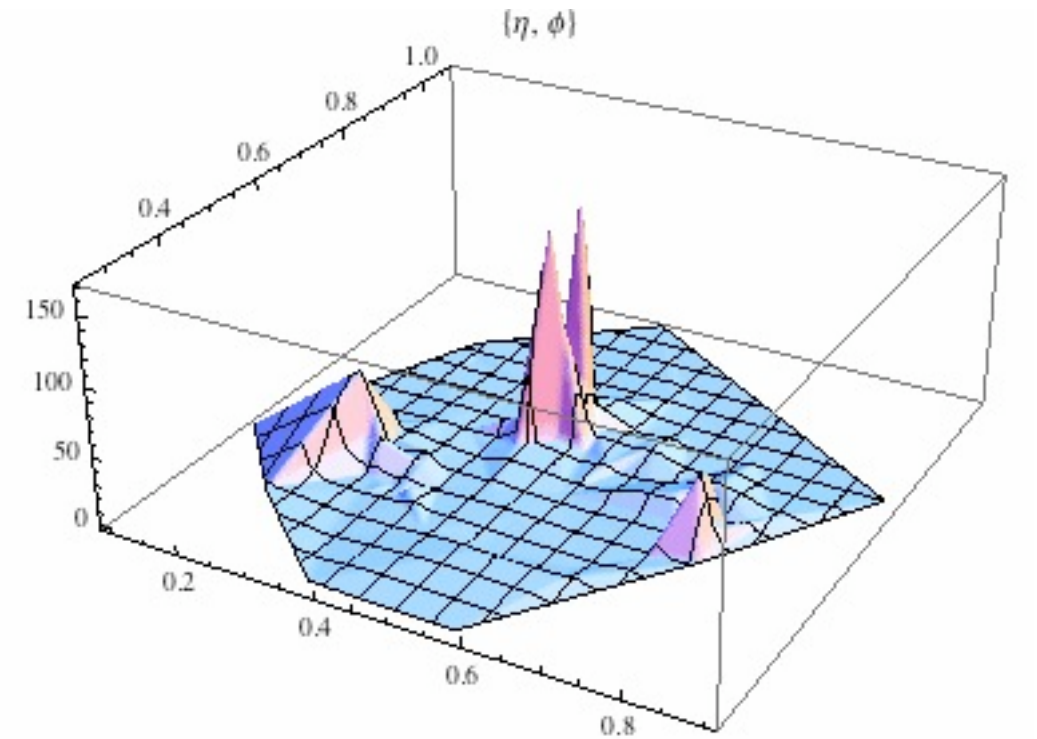

The Golden Triangle & events overlap

$$E^{b,q,\bar{q}}_{weighted}(\phi_b) = \int d\psi^J d\theta^J E^J(\theta^J, \psi^J)$$
$$\times \exp\left\{-\left[\frac{\theta^J(\psi^J) - \theta_{b,q,\bar{q}}}{\sqrt{2}\sigma_{\theta_{b,q,\bar{q}}}}\right]^2\right\} \exp\left\{-\left[\frac{\phi_{b,q,\bar{q}}(\phi_b) - \psi^J}{\sqrt{2}\sigma_{\phi_{b,q,\bar{q}}}}\right]^2\right\}$$

$$f = \int d\phi_b \exp\left\{-\left[\frac{E^b_{weighted}(\phi_b) - E_b}{\sqrt{2}\sigma_{E_b}}\right]^2\right\} \exp\left\{-\left[\frac{E^q_{weighted}(\phi_b) - E_q}{\sqrt{2}\sigma_{E_q}}\right]^2\right\}$$
$$\times \exp\left\{-\left[\frac{E^{\bar{q}}_{weighted}(\phi_b) - E_{\bar{q}}}{\sqrt{2}\sigma_{E_{\bar{q}}}}\right]^2\right\}$$

where $\theta_q = \theta_{\bar{q}} = \theta_b$ on the golden triangle, however $\phi_{b,q,\bar{q}}$ are not the same since the triangle is defined once ϕ_b is defined hence there is only a ϕ_b integral and $\phi_{q,\bar{q}}(\phi_b)$ are trivial functions of (ϕ_b) as we have calculated these on the triangle (and of course $\phi_b(\phi_b) = \phi_b$).

Conclusions

- LHC => new era, precision top physics.
- Calculation via PQCD, new insights.
  (not blindly dep' on MC).
- Side band: Improve significance.
- Substructures 2-B & 3-B.
- Complimentary methods, algorithms to interpolate between 3-jet/2jet/t-jets

Backups

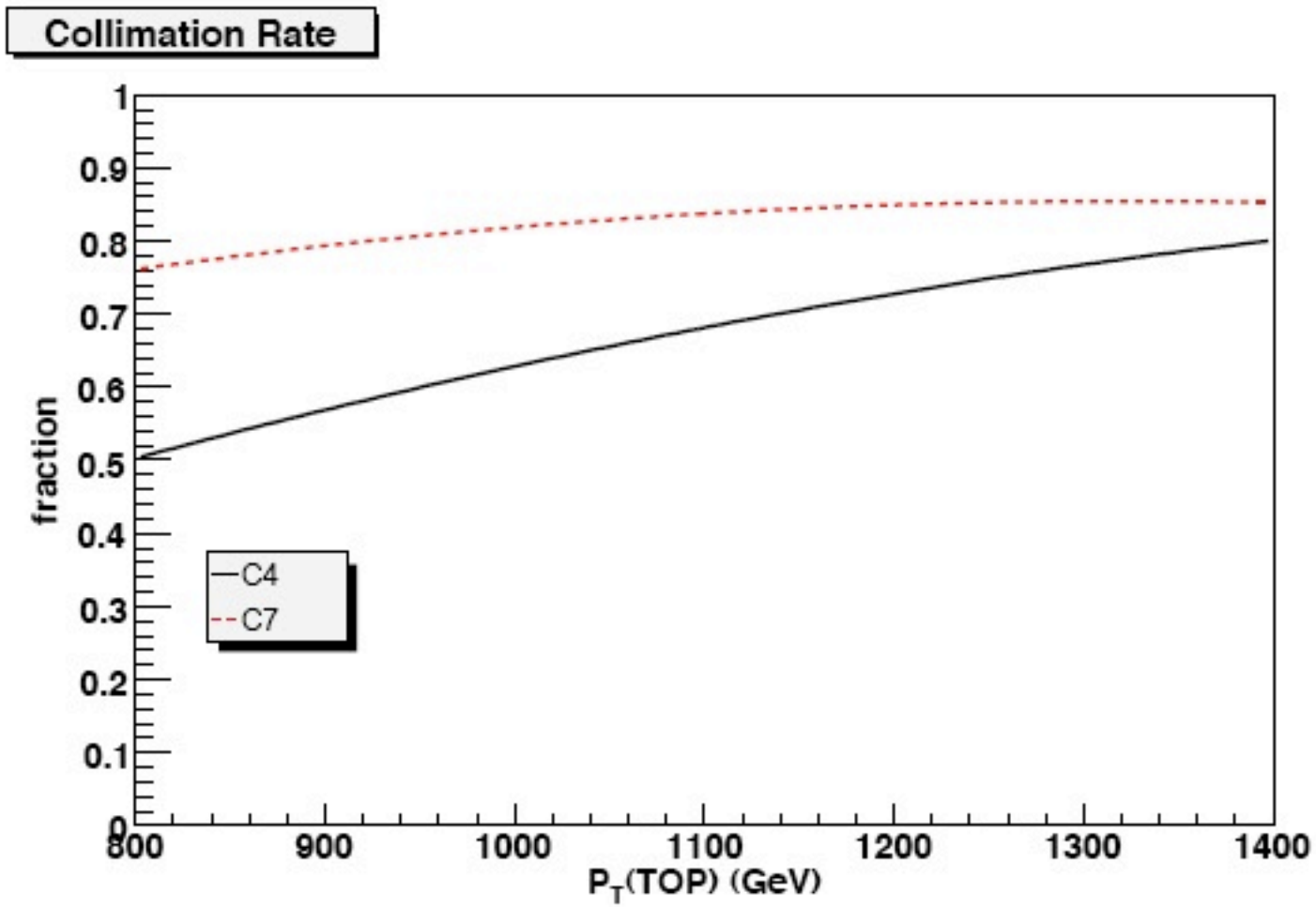

Figure 8: The collimation rate for top quarks as a function of their transverse momentum, for C4 (black solid curve) and C7 (red dashed curve) jets. Collimation rate is defined as the fraction of top quarks with $140\,\mathrm{GeV} \leq m_J \leq 210\,\mathrm{GeV}$.

Comparing jet function approx'

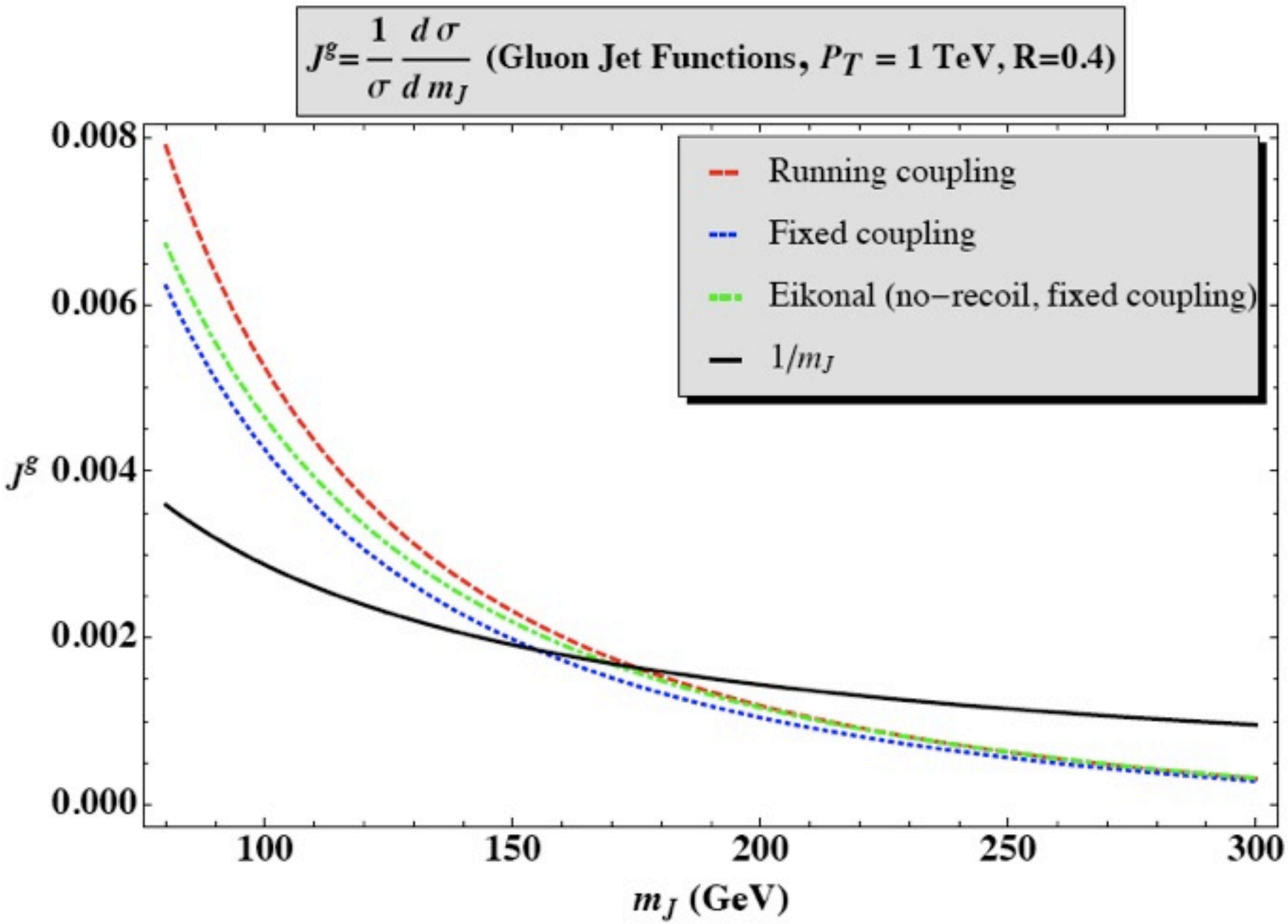

Jet mass distribution, theory vs. MC

Various MCs, at fixed p_T

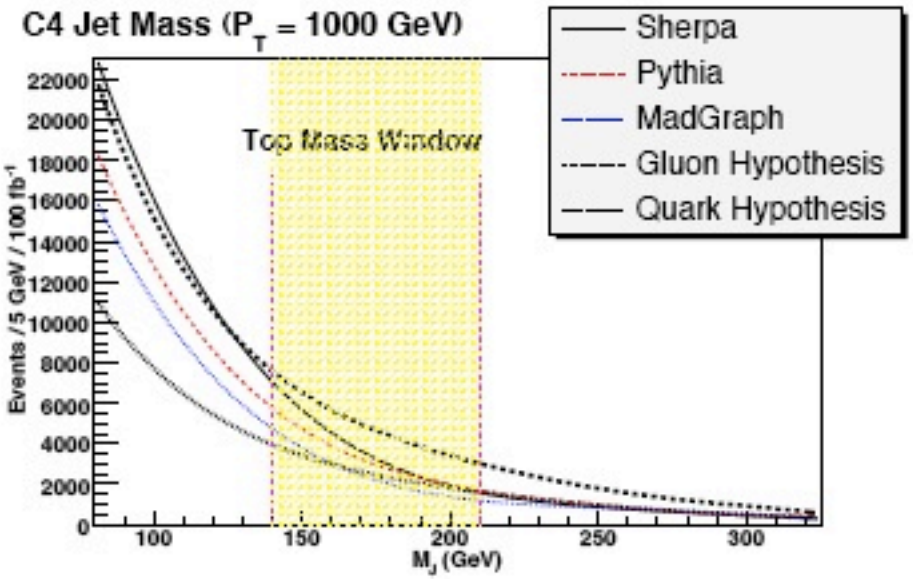

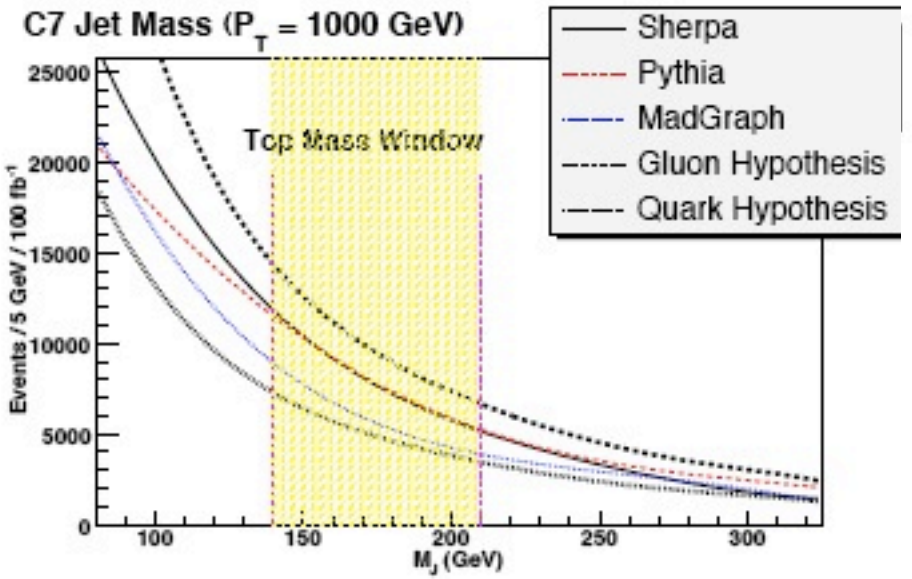

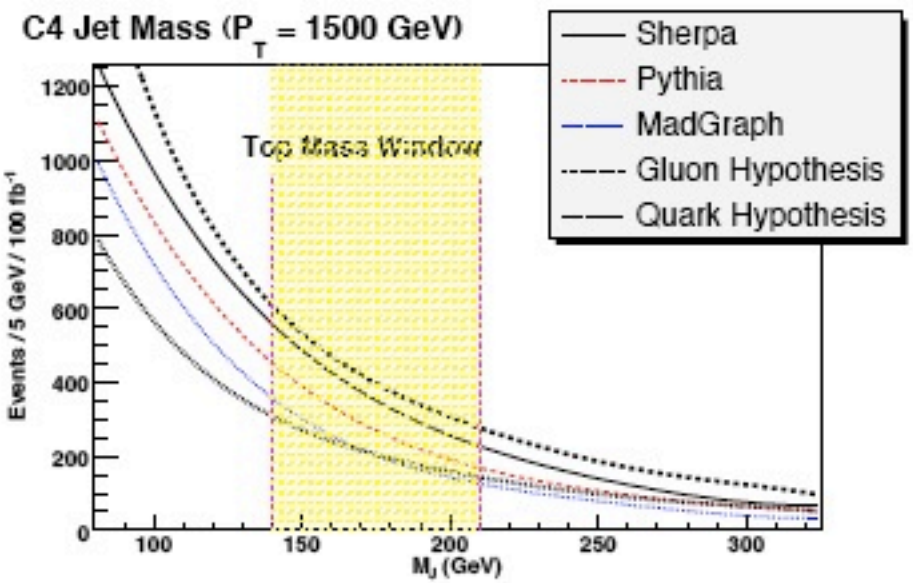

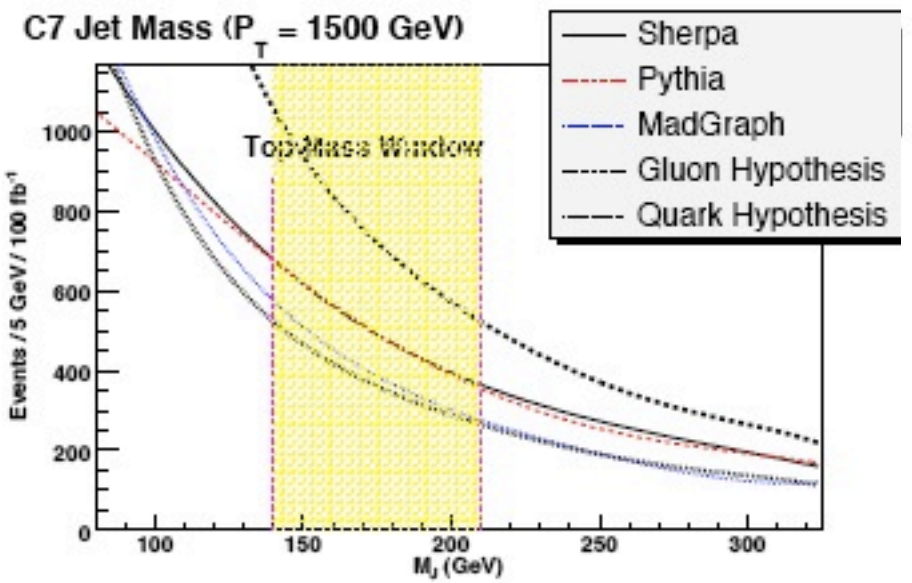

Pseudo-rapidity independence

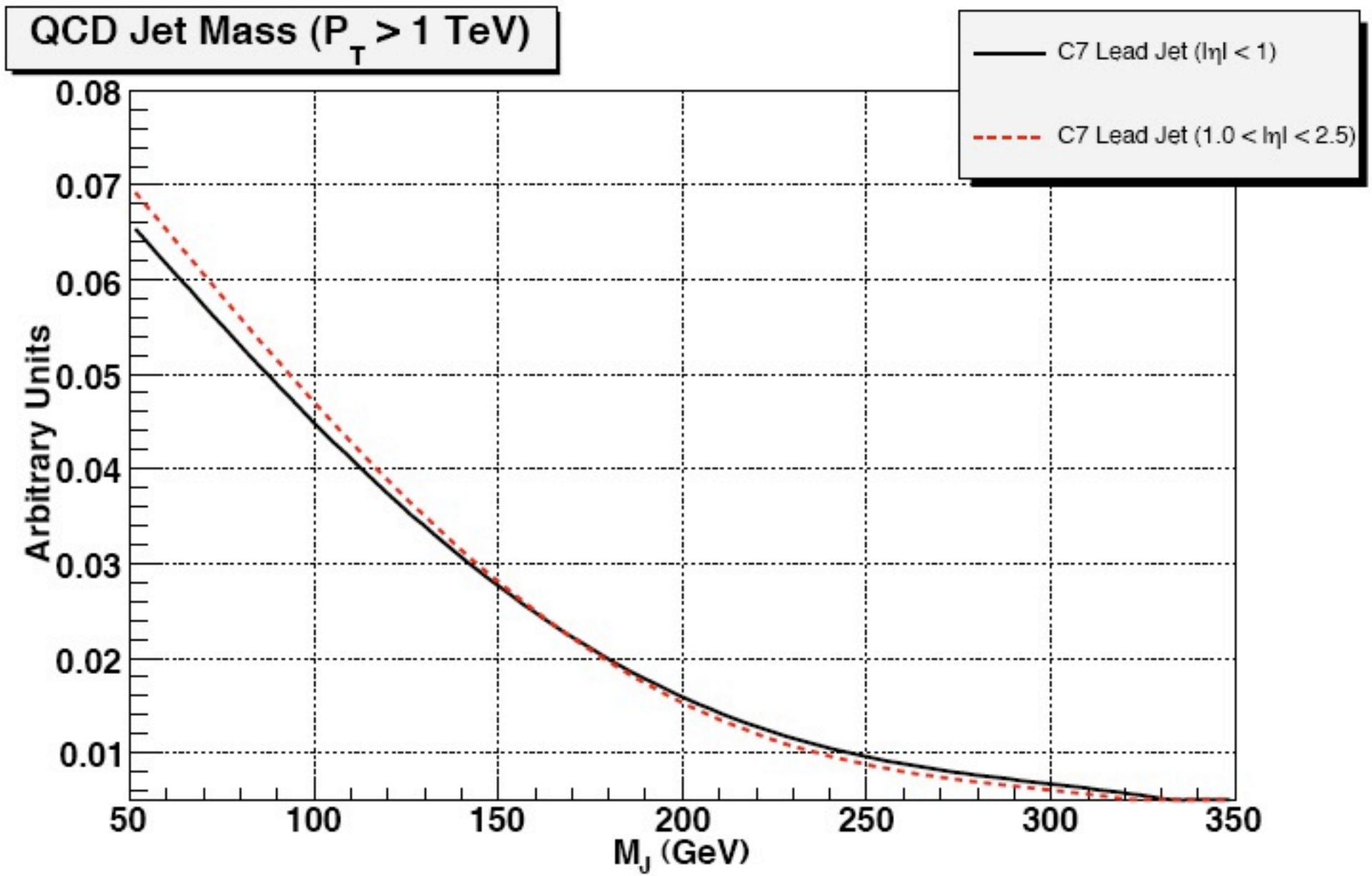

Bound fake rate (# of jets in top mass window)

$$\int_{140\ GeV}^{210\ GeV} dm_J\, J^q(m_J, p_T, R) \leq \text{ Fractional fake rate } \leq \int_{140\ GeV}^{210\ GeV} dm_J\, J^g(m_J, p_T, R)\,.$$

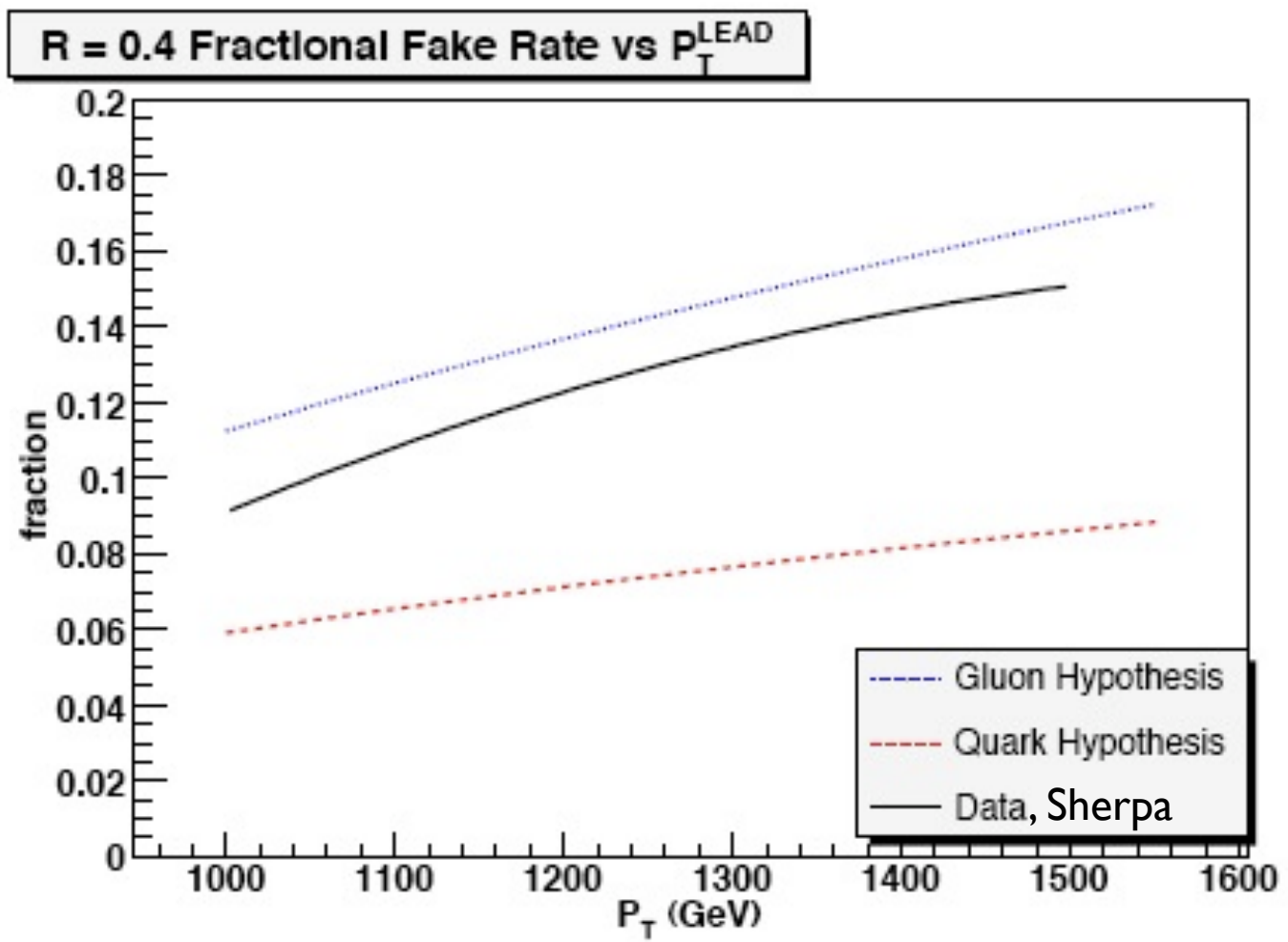

Results for leading jet, side band

For the subleading jet we simply require mass cut (no p_T cut)

$p_T{}^{lead} \geq 1500\,\mathrm{GeV}$ Cone $R = 0.4$ $100\ \mathrm{fb}^{-1}$

JES	B_{FIT}	S_{FIT}	ΔS	n_σ	p-value	χ^2/ndf	$(S/B)_{\mathrm{FIT}}$
0%	2341	430	94	4.6	0.99	0.35	0.184
5%	2968	624	110	5.7	0.96	0.45	0.210
-5%	1593	436	79	5.5	0.82	0.66	0.274

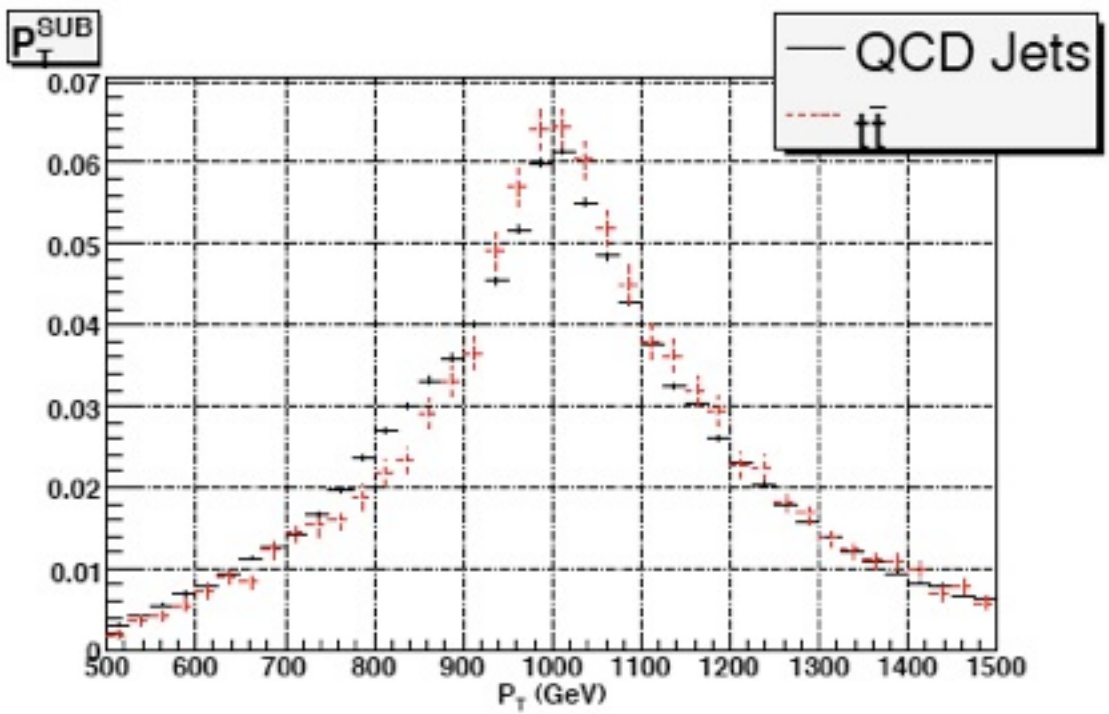

Angularity vs. Ysplitter

Once m_j, p_T are fixed then 2 body kinematics is characterized by a single variable

$$m_J^2 \sim p_{\rm min}(p_T - p_{\rm min})\Delta R^2/2\,, \quad Y_{12} = p_{\rm min}^2 \frac{\Delta R^2}{m_J^2}$$

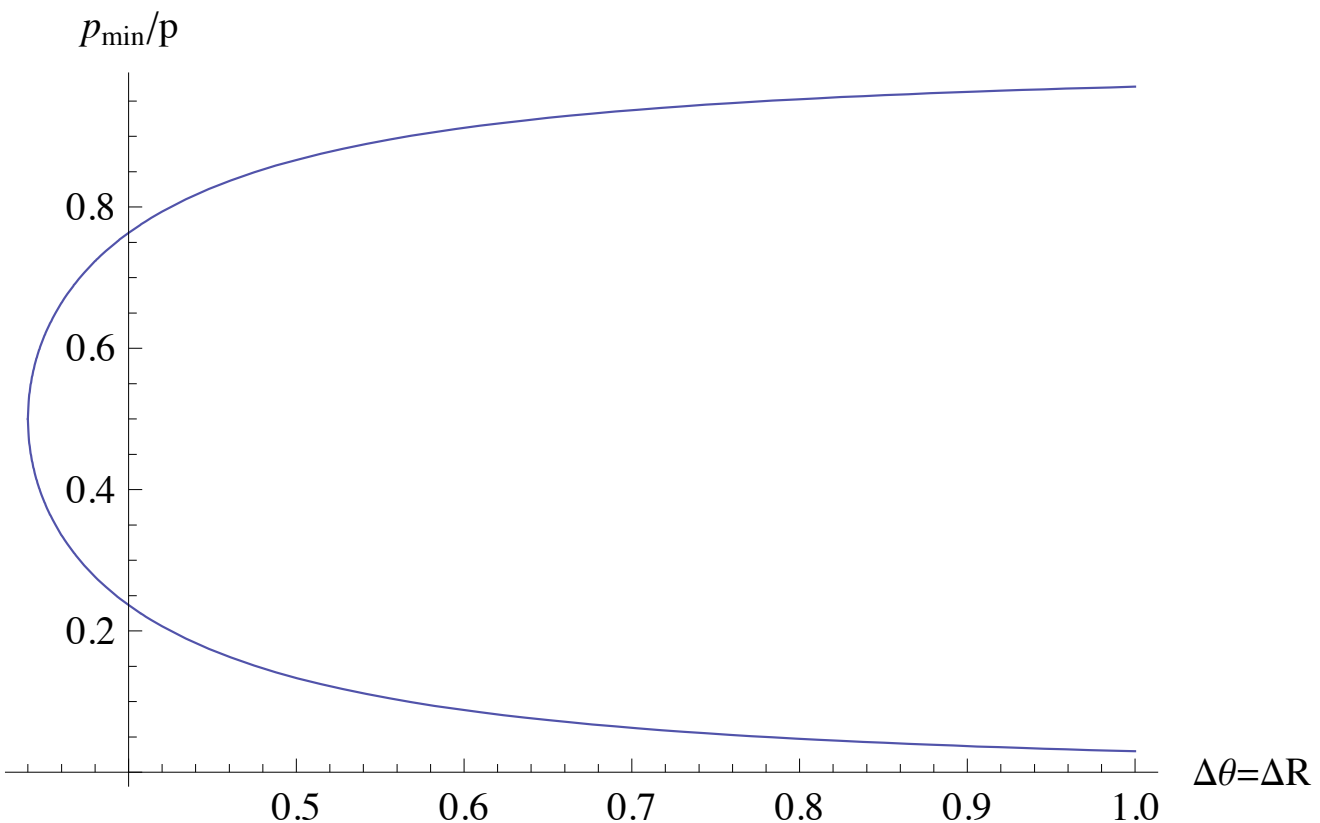

The challenge of highly boosted tops

The challenge of highly boosted tops

- Above a TeV, due to collimation, top's similar to light jet, efficiency & fake rate worsen.

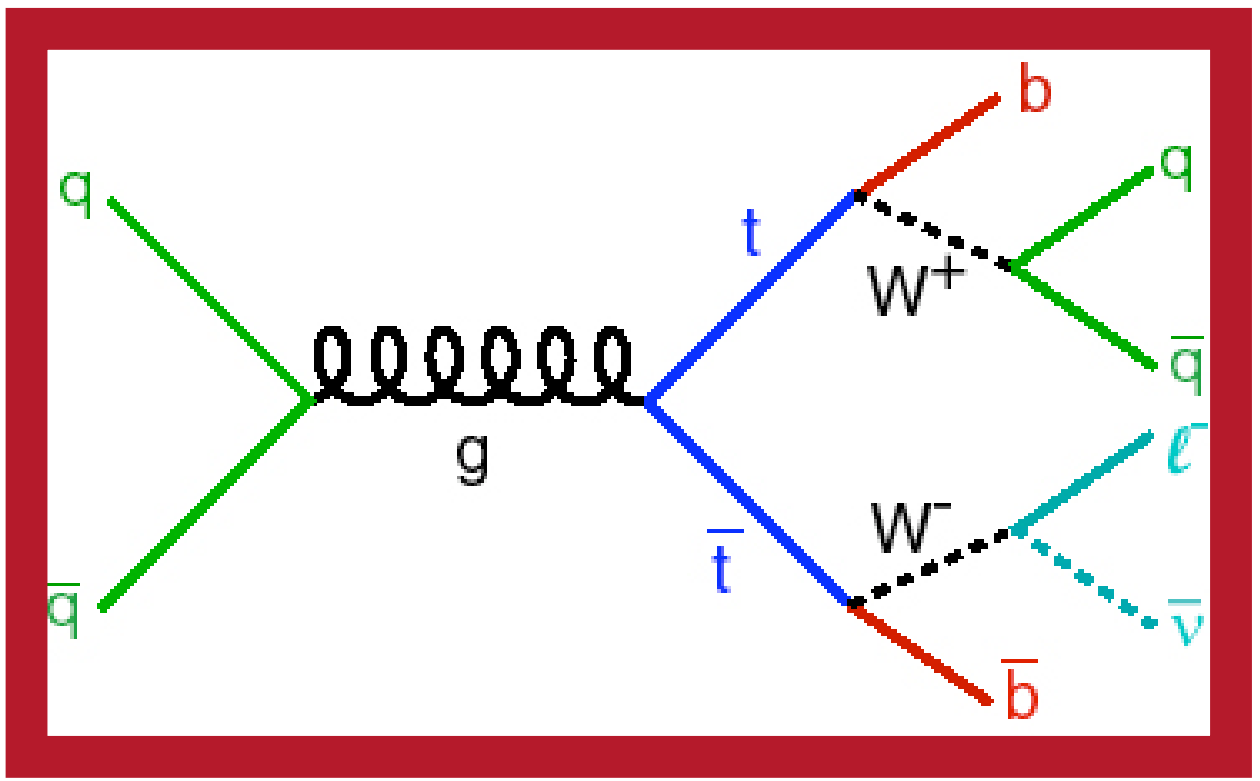

The challenge of highly boosted tops

- Above a TeV, due to collimation, top's similar to light jet, efficiency & fake rate worsen.

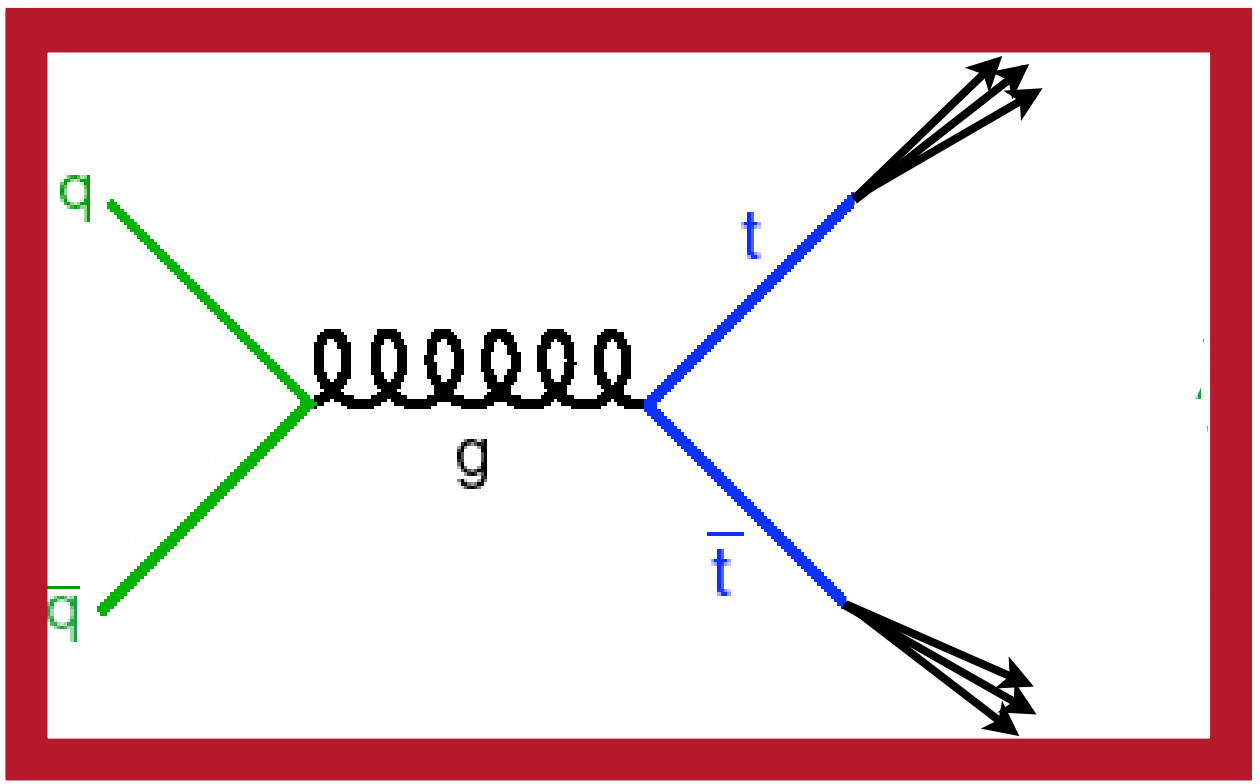

- The concept of top jet emerges.

Boosted top jets & collimation

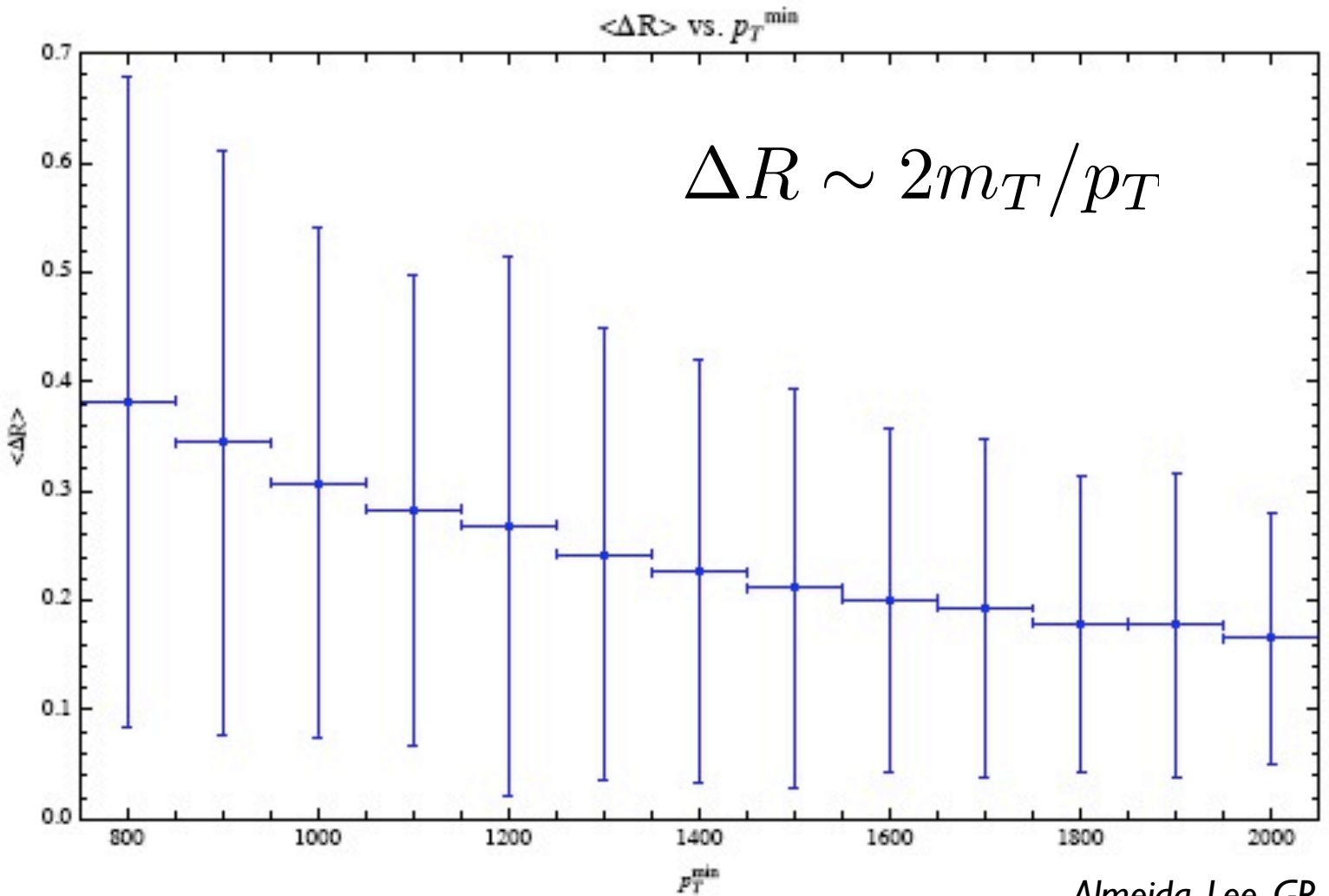

Almeida, Lee, GP, Sung & Virzi (08).

Highly Boosted Tops:
High Collimations!

ΔR vs. P_T